

# The Pleckstrin Homology Domain Proteins Slm1 and Slm2 Are Required for Actin Cytoskeleton Organization in Yeast and Bind Phosphatidylinositol-4,5-Bisphosphate and TORC2<sup>□</sup>

Maria Fadri,\* Alexes Daquinag,\* Shimei Wang, Tao Xue, and Jeannette Kunz

Department of Molecular Physiology and Biophysics, Baylor College of Medicine, Houston, TX 77030

Submitted July 7, 2004; Accepted January 25, 2005  
Monitoring Editor: Sandra Schmid

Phosphatidylinositol-4,5-bisphosphate [PtdIns(4,5)P<sub>2</sub>] is a key second messenger that regulates actin and membrane dynamics, as well as other cellular processes. Many of the effects of PtdIns(4,5)P<sub>2</sub> are mediated by binding to effector proteins that contain a pleckstrin homology (PH) domain. Here, we identify two novel effectors of PtdIns(4,5)P<sub>2</sub> in the budding yeast *Saccharomyces cerevisiae*: the PH domain containing protein Slm1 and its homolog Slm2. Slm1 and Slm2 serve redundant roles essential for cell growth and actin cytoskeleton polarization. Slm1 and Slm2 bind PtdIns(4,5)P<sub>2</sub> through their PH domains. In addition, Slm1 and Slm2 physically interact with Avo2 and Bit61, two components of the TORC2 signaling complex, which mediates Tor2 signaling to the actin cytoskeleton. Together, these interactions coordinately regulate Slm1 targeting to the plasma membrane. Our results thus identify two novel effectors of PtdIns(4,5)P<sub>2</sub> regulating cell growth and actin organization and suggest that Slm1 and Slm2 integrate inputs from the PtdIns(4,5)P<sub>2</sub> and TORC2 to modulate polarized actin assembly and growth.

## INTRODUCTION

Proteins involved in the regulation of cell signaling and membrane trafficking are often targeted to specific cell membranes in response to the synthesis of phosphoinositide second messengers. Seven different phosphorylated derivatives of phosphatidylinositol (PI) are currently known to exist in mammalian cells (Odorizzi *et al.*, 2000). These are phosphorylated at a single or multiple sites on the inositol head group of PI by an array of different phosphoinositide kinases (Fruman *et al.*, 1998). Besides serving as intermediates for the synthesis of other lipid second messengers, most if not all of the seven phosphoinositide species can act directly as second messengers and control the activation and membrane recruitment of effector proteins through binding to specific domains such as the pleckstrin homology (PH), FYVE, Phox, and epsin N-terminal homology domains (Hurley and Meyer, 2001; Lemmon, 2003; Cozier *et al.*, 2004).

From the various phosphoinositide second messengers, phosphatidylinositol-4,5-bisphosphate [PtdIns(4,5)P<sub>2</sub>] occupies a central position in lipid signaling pathways. PtdIns(4,5)P<sub>2</sub> is generated in all eukaryotic cells and regulates a diverse spectrum of cellular processes, including cytoskeletal reorganization, membrane trafficking, cell growth, apoptotic regulation, and ion channel activation

(Martin, 2001; Takenawa and Itoh, 2001; Yin and Janmey, 2003; Itoh and Takenawa, 2004). Previously, PtdIns(4,5)P<sub>2</sub> was considered to be only an intermediate in the generation of diacylglycerol, inositol-(1,4,5)-trisphosphate, and phosphatidylinositol-3,4,5-trisphosphate (Toker and Cantley, 1997; Toker, 1998). However, recent data show that PtdIns(4,5)P<sub>2</sub> is an important regulatory molecule in its own right that controls the activation and membrane recruitment of diverse PtdIns(4,5)P<sub>2</sub> binding proteins (Hurley and Meyer, 2001; Yin and Janmey, 2003). Many of these contain PtdIns(4,5)P<sub>2</sub>-binding modules, such as the PH domain, an ~120-amino acid protein domain found in proteins involved in signal transduction, actin organization, and membrane trafficking (Lemmon, 2003; Cozier *et al.*, 2004).

PtdIns(4,5)P<sub>2</sub> is a relatively abundant molecule that is enriched in the plasma membrane of all cells tested, ranging from organisms as diverse as yeast and human. Although the number of identified proteins that can bind PtdIns(4,5)P<sub>2</sub> in vitro has grown dramatically over the past years, it is still poorly understood how different pathways use this generic signaling molecule to specifically regulate many different cellular processes.

The phosphoinositide kinases and the pathway that generates PtdIns(4,5)P<sub>2</sub> are evolutionarily conserved. Therefore, genetically tractable systems such as the budding yeast *Saccharomyces cerevisiae* offer powerful tools to investigate PtdIns(4,5)P<sub>2</sub> signaling mechanisms on a genome-wide scale. In yeast, as in mammalian cells, PtdIns(4,5)P<sub>2</sub> is synthesized via the sequential phosphorylation of PI to phosphatidylinositol 4-phosphate [PtdIns(4)P] and PtdIns(4,5)P<sub>2</sub> through the action of PI 4-kinases and PtdIns(4)P 5-kinases, respectively (Fruman *et al.*, 1998; Odorizzi *et al.*, 2000). *S. cerevisiae* has a single and essential PtdIns(4)P 5-kinase, termed Mss4. Mss4p is localized to the plasma membrane and implicated in the regulation of cell cycle-dependent

This article was published online ahead of print in *MBC in Press* (<http://www.molbiolcell.org/cgi/doi/10.1091/mbc.E04-07-0564>) on February 2, 2005.

□ The online version of this article contains supplemental material at *MBC Online* (<http://www.molbiolcell.org>).

\* These authors contributed equally to this work.

Address correspondence to: Jeannette Kunz ([jkunz@bcm.tmc.edu](mailto:jkunz@bcm.tmc.edu)).

**Table 1.** *S. cerevisiae* strains used in this study

Strain	Genotype	Source
W303a	<i>MATa ade2-1 trp1-1 can1-100 leu2-3112 his3-11,15 ura3-1 GAL+</i>	Laboratory collection
W303 $\alpha$	<i>MATa ade2-1 trp1-1 can1-100 leu2-3112 his3-11,15 ura3-1 GAL+</i>	Laboratory collection
W303a/ $\alpha$	<i>MATa/MAT<math>\alpha</math> ade2-1/ade2-1 trp1-1/trp1-1 can1-100/can1-100 leu2-3112/leu2-3112 his3-11,15/his3-11,15 ura3-1/ura3-1 GAL+/GAL+</i>	Laboratory collection
JK9-3da	<i>MATa leu2-3112 ura3-52 rme1 trp1 his4 GAL HMLa</i>	Laboratory collection
BY4741	<i>MATa; his3<math>\Delta</math>1; leu2<math>\Delta</math>0; met15<math>\Delta</math>0; ura3<math>\Delta</math>0</i>	Laboratory collection
JK497	<i>Mata/MAT<math>\alpha</math> ade2-1 trp1 leu2-3112 his3-11,15 ura3 GAL+ mss4::HIS3MX6/MSS4</i>	This study
JK498	<i>W303<math>\alpha</math> pik1::KanMX carrying pRS314pik1-83</i>	This study
JK499	<i>W303<math>\alpha</math> mss4::HIS3MX6 carrying YCplac111::mss4-2ts</i>	This study
JK502	<i>W303a except slm1::KanMX</i>	This study
JK503	<i>W303<math>\alpha</math> except slm1::KanMX</i>	This study
JK504	<i>W303a except slm2::KanMX</i>	This study
JK505	<i>W303<math>\alpha</math> except slm2::KanMX</i>	This study
JK506	<i>W303a except slm2::HIS3</i>	This study
JK507	<i>W303a/<math>\alpha</math> except slm1::KanMX/SLM1 slm2::HIS3/SLM2</i>	This study
JK508	<i>W303a except slm1::KanMX/SLM1 slm2::HIS3/SLM2 carrying pJK702</i>	This study
JK509	<i>W303<math>\alpha</math> except slm1::KanMX/SLM1 slm2::HIS3/SLM2 carrying pJK703</i>	This study
JK510	<i>W303a except SLM2-GFP::HIS3MX6</i>	This study
JK511	<i>MATa ade2-1 trp1 leu2-3112 his3-11,15 ura3 GAL+ mss4::HIS3MX6 ura3-52::mss4-2ts-URA3</i>	This study
JK512	<i>W303a except slm1::KanMX slm2::HIS3 carrying pJK702</i>	This study
JK513	<i>W303<math>\alpha</math> except slm1::KanMX slm2::HIS3 carrying pJK703</i>	This study
JK514	<i>JK9-3da except fab1-2; obtained by backcrossing strain (Yamamoto <i>et al.</i>, 1995) twice with JK9-3d</i>	This study
JK515	<i>W303a except slm1::KanMX slm2::HIS3 carrying pSW4</i>	This study
JK516	<i>W303a except slm1::KanMX slm2::HIS3 carrying pSW5</i>	This study
JK517	<i>W303a except bit61::HIS3MX avo2::KanMX</i>	This study
JK518	<i>JK515 except inp51::LEU2</i>	This study
YJC1426	<i>MATa ade2 ade3 ura3 leu2 trp1 lys2 stt4-7-LEU2</i>	Muhua <i>et al.</i> (1998)
95700	<i>BY4741 except SLM1-GFP-URA3</i>	Research Genetics
7502123	<i>BY4741 except AVO2-TAP-HIS3</i>	Open Biosystems
7501161	<i>BY4741 except BIT61-TAP-HIS3</i>	Open Biosystems

actin reorganization (Desrivieres *et al.*, 1998; Homma *et al.*, 1998).

PtdIns(4,5)P<sub>2</sub> generated by Mss4 is thought to mediate many of its cellular functions by inducing the plasma membrane recruitment and activation of proteins containing PH domains. For example, PtdIns(4,5)P<sub>2</sub> mediates the plasma membrane translocation of Rom2 by binding to its PH domain (Audhya and Emr, 2002). Rom2 is a GTP exchange factor that activates the partially redundant Rho1 and Rho2 GTPases, which in turn, regulate actin polarization, polarized secretion, endocytosis, and cell wall synthesis by signaling to multiple downstream effectors (Cabib *et al.*, 1998; deHart *et al.*, 2003; Dong *et al.*, 2003; Valdivia and Schekman, 2003). Known Rho1 effectors include the protein kinase C (PKC) (Pkc1) (Kamada *et al.*, 1996; Delley and Hall, 1999), the formin protein Bni1 (Kohno *et al.*, 1996), the  $\beta$ -1,3 glucan synthase Fks1 (Qadota *et al.*, 1996), the transcription factor Skn7 (Alberts *et al.*, 1998; Ketela *et al.*, 1999), and the exocyst complex component Sec3 (Guo *et al.*, 2001). Similarly, PtdIns(4,5)P<sub>2</sub> binds to the PH domains of the related Boi1 and Boi2 and thereby mediates their localization to the bud, which is important for their role in the regulation of polarized growth (Bender *et al.*, 1996; Hallett *et al.*, 2002). In addition, PtdIns(4,5)P<sub>2</sub> modulates nuclear migration during mitosis via interaction with the Num1 PH domain (Farkasovsky and Kuntzel, 1995) and controls the membrane recruitment and activation of phospholipase D 1 (PLD1/Spo14), whose function is important for secretion and cellular differentiation during meiosis (Sciorra *et al.*, 2002). Thus, diverse PH domain-containing proteins are critical effectors of PtdIns(4,5)P<sub>2</sub> that mediate key aspects of PtdIns(4,5)P<sub>2</sub> signaling.

To further our understanding of PtdIns(4,5)P<sub>2</sub> signaling, we wished to identify novel *in vivo* targets of PtdIns(4,5)P<sub>2</sub> and to elucidate the mechanism by which PtdIns(4,5)P<sub>2</sub> regulates their cellular functions. We took a candidate gene approach and analyzed the phosphoinositide binding properties of yeast proteins containing a PH domain. Here, we report on the characterization of two novel effectors of PtdIns(4,5)P<sub>2</sub>, encoded by homologous genes termed Synthetic lethal with MSS4 (*SLM1*) and *SLM2*. Slm1 and Slm2 function in a PtdIns(4,5)P<sub>2</sub>-regulated signaling branch that is required for cell growth and actin polarization. Slm1 localization to the plasma membrane is essential for its *in vivo* function and is modulated by interaction with PtdIns(4,5)P<sub>2</sub> and components of the TORC2 signaling complex. We propose that Slm1 and Slm2 function in a signaling network that integrate inputs from both the Mss4 and Tor2 pathways to elicit downstream responses required for actin polarization and cell growth.

## MATERIALS AND METHODS

### Materials, Strains, and Plasmids

Aprotinin, chymostatin, leupeptin, pepstatin, and phenylmethylsulfonyl fluoride (PMSF) were obtained from Sigma-Aldrich (St. Louis, MO). Geneticin (G418) and Pfx polymerase were from Invitrogen (Carlsbad, CA). Glutathione (GSH)-conjugated or Ni<sup>2+</sup>-conjugated agarose beads were from BD Biosciences Clontech (Palo Alto, CA). Mouse monoclonal anti-glutathione S-transferase (GST) antibodies were from Sigma-Aldrich, anti-hemagglutinin (HA) antibodies were from Babco (Richmond, CA), Cy2-conjugated goat anti-mouse IgG were from Jackson ImmunoResearch Laboratories (West Grove, PA), and Alexa-594-conjugated phalloidin was from Molecular Probes (Eugene, OR). Molecular mass standards were from Bio-Rad (Hercules, CA).

*S. cerevisiae* strains and plasmids used are listed in Table 1 and Table 2,

**Table 2.** Plasmids used in this study

Plasmid	Characteristic	Source
pAS24	YCplac111, <i>CEN</i> , <i>LEU2</i> , allows expression of proteins N-terminally tagged with a double HA-tag under the control of the <i>GAL1</i> promoter	Schmidt <i>et al.</i> (1997)
pAS25	YCplac33, <i>CEN</i> , <i>URA3</i> , allows expression of proteins N-terminally tagged with a 2 × HA-tag under the control of the <i>GAL1</i> promoter	A. Schmidt
pJK701	<i>HA-SLM1</i> in pAS24	This study
pJK702	<i>HA-SLM1</i> in pAS25	This study
pSW1	<i>HA-SLM2</i> in pAS24	This study
pJK703	<i>HA-SLM2</i> in pAS25	This study
pJK704	<i>HA-SLM1</i> <sub>ΔC</sub> in pAS25	This study
pJK705	<i>HA-SLM2</i> <sub>ΔC</sub> in pAS25	This study
pSW2	<i>HA-SLM1</i> <sub>ΔC</sub> in pAS24	This study
PSW4	<i>slm1-3</i> in p416GPD, <i>CEN</i> , <i>URA3</i>	This study
PSW5	<i>slm1-3</i> in p415GPD, <i>CEN</i> , <i>LEU2</i>	This study
pAD41	<i>HA-SLM1</i> <sub>M1</sub> in pAS25	This study
pAD42	<i>HA-SLM1</i> <sub>M2</sub> in pAS25	This study
pAD43	<i>HA-SLM2</i> <sub>M1</sub> in pAS25	This study
PJK706	<i>SLM1-PH</i> in pGEX5 × -1	This study
pAD44	<i>GST-SLM1-PH</i> <sub>M1</sub> in pGEX5 × -1	This study
pAD45	<i>GST-SLM1-PH</i> <sub>M2</sub> in pGEX5 × -1	This study
pJK708	<i>6HIS-SLM1</i> in pET28a (Novagen)	This study
pJK709	<i>6HIS-SLM2</i> in pET28a (Novagen)	This study
pJK710	<i>AVO2</i> in TNT521 (Udan <i>et al.</i> , 2003)	This study
pJK711	<i>BIT61</i> in TNT521	This study
pJK712	<i>YBR270C</i> in TNT521	This study
pC-186	Genomic fragment containing the <i>RHO1</i> gene, 2μ <i>URA3</i>	Madaule <i>et al.</i> (1987)
pRHO2	Genomic fragment containing the <i>RHO2</i> gene in Yeplac195, 2μ <i>ARS</i> , <i>URA3</i>	M. Hall
pPKC1	Genomic fragment containing <i>PKC1</i> in Yeplac195, 2μ <i>ARS</i> , <i>URA3</i>	M. Hall
pPKC1(R398P)	<i>Ycp50</i> , <i>URA3</i> , <i>CEN</i> containing the dominant active allele <i>PKC1(R398P)</i>	Levin <i>et al.</i> (1990)
pBCK1	Genomic fragment containing <i>BCK1</i> in pRS314, <i>TRP1</i> , <i>CEN</i>	Lee and Levin (1992)
pBCK1-20	Genomic fragment containing the dominant active allele <i>BCK1-20</i> in pRS314, <i>TRP1</i> , <i>CEN</i>	Lee and Levin (1992)
pDLB824	<i>CEN HA-MKK1DD</i> ; constitutively activated <i>MKK1-DD</i> mutant, altering residues Ser-377 and Thr-381 to Asp	Harrison <i>et al.</i> (2004)
pMPK1	Genomic fragment containing <i>HA-MPK1</i> in <i>Ycp50</i> ( <i>CEN</i> , <i>URA3</i> )	M. Gustin
pHA-TOR2	2 × HA-tagged <i>TOR2</i> in pAS25	Kunz <i>et al.</i> (2000)
pHA-TOR2-KD	2 × HA-tagged <i>TOR2</i> kinase-dead mutant in pAS25	Kunz <i>et al.</i> (2000)
PGAL1-SigD	<i>SigD</i> ORF under control of the <i>GAL1</i> promoter in pTB227 ( <i>URA3</i> , <i>CEN</i> ; Kunz <i>et al.</i> , 2000)	This study

respectively. To construct temperature-sensitive strains, plasmids containing the temperature-sensitive *pik1-83* and *mss4-2* alleles were isolated from strains AAY104 and SD102 (Desrivieres *et al.*, 1998; Foti *et al.*, 2001), respectively, and transferred into heterozygous *pik1Δ* or *mss4Δ* deletion strains generated by transformation of the diploid W303 a/α strain with polymerase chain reaction (PCR) products containing *pik1::KanMX* (Open Biosystems, Huntsville, AL) and *mss4::HIS3MX6* (from strain JK497) disruption alleles. Haploid segregants harboring the appropriate markers were obtained by sporulation and dissection of the diploid strains. For generation of double-mutant strains, single-mutant strains of opposite mating types were first mated and sporulated. Tetrads were then dissected, and segregants containing the appropriate markers were selected. To construct the haploid yeast strains harboring the *slm1Δ slm2Δ* and carrying plasmid-borne *SLM1* or *SLM2* genes, strains JK508 and JK509, respectively, were induced to sporulate, and tetrads were dissected onto YPG medium. Segregants were then selected for the presence of the appropriate markers. Yeast strains in the BY4741 strain background containing C-terminally green fluorescent protein (GFP)-tagged *Slm1* or tandem affinity procedure (TAP)-tagged *Avo2*, *Bit61* were purchased from Research Genetics (Invitrogen).

### General Genetic Manipulations

Wild-type yeast strains were grown at 30°C, whereas temperature-sensitive mutants were maintained at 26°C unless otherwise indicated. Media were described previously (Sherman *et al.*, 1983). Strain construction followed standard methods (Sherman *et al.*, 1983). Yeast cells were transformed by the lithium acetate procedure (Ito *et al.*, 1983), and transformants were selected on SD medium lacking the appropriate amino acid supplement for maintenance of the plasmid marker.

### Cloning of Expression Constructs and Generation of Truncation and Point Mutants

*SLM1*, *SLM2*, *AVO2*, *BIT61*, and *YBR270C* open reading frames (ORFs) and ~200-base pair flanking regions downstream of the stop codon were PCR

amplified using Pfx polymerase from genomic DNA isolated from strain JK9-3D by using the following primers: *SLM1-FOR* 5'-CTACTACTCGAGAT-GTCGAAAAACAACAATG and *SLM1-REV* 5'-CTACTACTCGAGCTTCATCCATGCATGGGACACA; *SLM2-FOR* 5'-CTACTACTCGAGATGCTTACCAACG-GAACAG *SLM2-REV* 5'-CTACTACTCGAGACCAGCAGTATTCATTTGATATAA; *AVO2-FOR* 5'-GTCGTAGGATCCATGTTGAAAGAGCCCTCAGTTC and *AVO2-REV* 5'-GTAGTAGTCGACGAAGAACGCATCTCAGTGG; *BIT61-FOR* 5'-GTAG-TAAGATCTATGACAGCAGAAGATATACTCC and *BIT61-REV* 5'-GTAGTA-AGATCTGCTGTGTCATCGCTGATTC; and *YBR270C-FOR* 5'-GTAGTA-AGATCTATGGCAACAGACCTAAATCGTA and *YBR270C-REV* 5'-GTAG-TACTCGAGGTTCTTTCTGACTCTTAGCAAG. The PCR reactions were digested with appropriate restriction enzymes (recognition site incorporated into the primer sequences; underlined in primer sequence) and cloned into various expression vectors. The *SLM1*<sub>ΔC</sub> and *SLM2*<sub>ΔC</sub> truncation mutants were generated by PCR amplification by using Pfx polymerase and *SLM1* or *SLM2* DNA as template with the following primers: *SLM1-FOR* and *SLM1ΔC-REV* (5'-CTACTACTCGAGTTATGTCCTCATCGGTAGATTAGG); *SLM2-FOR* and *SLM2ΔC-REV* (5'-CTACTACTCGAGTTAAGGATCGTCTTTGATTGCTA). The *Slm1* PH domain expression construct was generated using primers *SLM1PH-FOR* 5'-CTTCAATTC AAGGGATCCCAAC in combination with *SLM1-REV*. The resulting PCR fragment was cloned as a *Bam*HI-*Xho*I fragment into the *Escherichia coli* expression vector pGEX5 × -1 (Pfizer, New York, NY). The *SLM* point mutants were constructed using the QuikChange site-directed mutagenesis kit (Stratagene, La Jolla, CA). Site-directed mutagenesis on *SLM1* and *SLM2* was performed according to the manufacturer's instructions by using gene-specific primers containing the desired codon changes incorporated. Primers were *SLM1-M1FOR* 5'-ATTTCTAAACCTC-TAATCAAACGGGTATTATGTG; *SLM1-M1REV* 5'-CACATAATACCCGTTT-GAATAGGAGTTTGAAGAAAT; *SLM1-M2FOR* 5'-ATCAGGGTTTTAGAAAA-CAACTCAAAAATTTCTAAA; *SLM1-M2REV* 5'-GGAGTTTAAAAATTTGAGTTT-G TTTTCTAAAACCC; *SLM2-M1FOR* 5'-AATTTTTAAACTATACTCAAAAT-GGGTTTTATGTCC; *SLM2-M1REV* 5'-GGACATAAAAACCCATTTGAGTATGA-GTTTTAAAAAT; and *SLM2-M2FOR* 5'-ATCTGGGTTTCTGGAGAACAAC-TCAAAAATTTTTAAA; *SLM2-M2REV* 5'-GAGTTTTAAAAATTTGAGTTGTTCTC-

CAGAAACCCA. The successful construction of all constructs and mutants with only the desired changes was confirmed by DNA sequence analysis.

### Gene Disruptions

All gene disruptions, except when noted otherwise, were generated using DNA fragments containing *KanMX2* disruption cassettes of each individual gene and 300-base pair upstream and downstream flanking regions. The disruption cassettes were PCR amplified from genomic DNA generated from strains in the S288C background and containing single genomic deletion disruptions (purchased from Open Biosystems). The PCR reactions were transformed into the diploid strain W303a/ $\alpha$  for one-step gene replacement and G418-resistant transformants were selected. The disruptions were confirmed by PCR with the use of three different sets of primers. The *slm2::HIS3* deletion allele was constructed by first cloning the 2.3-kb *XhoI* fragment containing the entire *SLM2* ORF and 220 base pairs downstream of the stop codon into the *SalI* site of plasmid pGem5zf (Promega, Madison, WI) to generate pGem5zf-*SLM2*. The internal 0.6-kb *BamHI*-*BglIII* fragment of pGem5zf-*SLM2* was then replaced with a *BamHI* cassette containing the *Schizosaccharomyces pombe HIS5* gene (complements a *S. cerevisiae his3* mutant) PCR amplified from plasmid pFA6a-*HIS3MX* (Longtine *et al.*, 1998). A *NotI*-*SpeI* fragment of pGem5zf-*slm2::HIS3* was transformed into strain W303a/ $\alpha$  for one-step gene replacement, and His<sup>+</sup> transformants were selected and confirmed by PCR. To construct the *bit61::HIS3* mutant, the internal 1.6-kb *BamHI* fragment in vector pGem5zf-*BIT61* was replaced by a *BamHI* restriction fragment containing *HIS3MX*. The resulting *bit61::HIS3MX* cassette was cut with *SphI* and *SacI* and transformed into yeast strain W303a for one-step gene replacement, and His<sup>+</sup> transformants were selected and confirmed by PCR.

### Synthetic Lethal Analysis

Doubly heterozygous diploids were generated by crossing haploid strains and selecting for the presence of appropriate markers. To obtain *slm1 $\Delta$  stt4-7* double mutants the *slm1::KanMX* strain JK503 was mated with strain YJ1426. The *slm1::KanMX* mutation was combined with the *mss4-2* temperature-sensitive mutation by mating strains JK503 and JK511. The *stt4-7-LEU2* and *mss4-2-URA3* mutant strains JK503 and JK511 also were mated to strain JK505 containing a null mutation in *SLM2* (*slm2::KanMX*). Diploids were sporulated at 26°C, and tetrads were dissected and allowed to germinate at 26°C on YEPD medium and scored for G418 resistance or the presence of auxotrophic markers. For *slm1 $\Delta$  stt4-7* genetic analysis, 53 tetrads were dissected (PD:TT: NPD = 9:36:8). Of the expected 52 double mutant segregants, none was recovered. For *slm2 $\Delta$  stt4-7* genetic analysis 22 tetrads were dissected (PD:TT: NPD = 6:12:4). Of the expected 20 double mutant segregants, 13 were recovered. For the analysis of *slm1 $\Delta$  mss4::HIS3 ura3-52::mss4-2:URA3* mutants 47 tetrads were dissected. Of the expected 23 G418<sup>R</sup> Ura<sup>+</sup> His<sup>+</sup> segregants, none was recovered, whereas 11 G418<sup>R</sup> Ura<sup>+</sup> segregants and nine His<sup>+</sup> Ura<sup>+</sup> segregants were isolated. For *slm2 $\Delta$  mss4::HIS3 ura3-52::mss4-2:URA3*, a total of 32 tetrads were dissected, of the expected 35 G418<sup>R</sup> Ura<sup>+</sup> His<sup>+</sup> segregants, 12 were recovered.

### Expression and Purification of Proteins in *E. coli*

All proteins were expressed in *E. coli* BL21( $\lambda$ DE3) as GST or 6His fusion proteins and purified on GSH-conjugated and Ni<sup>2+</sup>-chelating agarose beads, respectively, following the manufacturer's instructions.

### Protein Lipid Overlay Assay

Overlay assays were performed as described previously (Dowler *et al.*, 2002) by using prespotted PIP Strip membranes (Echelon Biosciences, Salt Lake City, UT). Membranes were incubated overnight at 4°C with 500 ng/ml purified recombinant GST or GST fusion protein. Bound GST fusion proteins were detected by Western blot with anti-GST antibodies (1:2000 dilution) followed by horseradish peroxidase-coupled goat anti-rabbit antibody (1:25,000 dilution) as described previously (Dowler *et al.*, 2002).

### Microscopy

To localize HA-Slm1 or HA-Slm2 proteins, plasmids containing wild-type *SLM1*, *SLM2*, or mutated variants thereof were transformed into the wild-type yeast strain W303a or strains containing temperature-sensitive mutations (together with their wild-type controls). These plasmids expressed the different *SLM* variants in yeast under the control of the *GAL1* promoter as a fusion protein with a double HA epitope at the N terminus. The HA-tagged Slm1 and Slm2 proteins were both functional, because they complemented the growth defects of a *slm1 $\Delta$  slm2 $\Delta$*  double mutant. Liquid cultures were grown in selective raffinose medium at 25°C to early log phase, galactose (2%) was added to induce expression of HA-*SLM1* and HA-*SLM2* and incubation was continued at either 25 or 38°C for 1.5 h. Expression of HA-Slm1 was verified and quantitated by Western blot analysis of cell extracts. HA-Slm1 protein levels were comparable in wild-type and lipid kinase mutant strains assayed under the same condition, except in the *fab1-2* strain background, which generally yielded somewhat lower levels of protein expression from the *GAL1* promoter.

Cells were fixed for immunofluorescence experiments by addition of 1/10 1 M potassium phosphate buffer, pH 6.9, and formaldehyde solution (4% final concentration) directly to the media and incubation for 3–4 h shaking at room temperature (RT). Cells were then collected by centrifugation, washed, spheroblashed, permeabilized, and incubated with primary (mouse monoclonal HA-11 anti-HA) and secondary (Cy2-conjugated goat anti-rabbit IgG) as well as Alexa-594-conjugated phalloidin. Slm1-GFP experiments were performed using cells grown in selective media (selecting for maintenance of chromosomally encoded or plasmid-borne GFP fusions), diluted into SD complete medium for 2 h and mounted for viewing in 1% low-melting agarose.

Cdc42 was visualized essentially as described previously (Richman *et al.*, 2002). Cells of strain JK515, transformed with plasmid p415MET-GFP-CDC42, were grown in SD-Leu medium to mid-log phase, diluted into SD-Met-Leu medium for expression of the methionine-repressible promoter, and incubated for 1 h at 25°C followed by 2 h at either RT or 38°C. To visualize Rho1, the plasmid pRB2138-GFP-RHO1 was introduced into strain JK516. Transformants were grown in SD-Ura medium to mid-log phase at RT and for additional 2–3 h at either RT or 38°C. GFP fusion proteins were visualized by fluorescence microscopy in living cells, mounted for viewing in 1% low-melting agarose.

All cells were viewed using a 100 $\times$  plan oil-immersion lens (numerical aperture 1.4). Images were acquired with the use of a DeltaVision deconvolution microscope (Applied Precision, Mississauga, Ontario, Canada). Z series stacks were created by sequentially scanning green and red channels at 0.5- $\mu$ m steps by using 2  $\times$  binning. For the quantitation of HA-Slm1 localization, Z series were collected from cells grown under the same growth conditions by using identical gain and exposure times. Images were deconvoluted using the Deltavision software and were then exported as Tiff files and processed with the use of Adobe Photoshop 6.0. Heightfield visualizations were performed on single z-sections of representative cells by using Amira 3.0 (Indeed Visual Concepts, Berlin, Germany). Single confocal sections were obtained from the middle of cells using a Zeiss LSM510 confocal laser scanning microscope. Density plots were generated using NIH Image 1.62. Pixel intensity was determined by a "raw average plot" from four to six cells.

### Scoring of Cytoskeletal Polarization and Polarized Distribution of Marker Proteins

Actin polarization was examined in small- and medium-budded cells (~100 cells analyzed in each case). The actin cytoskeleton was considered polarized if six or fewer actin patches were localized in the mother cells and patches were concentrated at the bud neck and actin cables were polarized. Cells with the majority of actin patches polarized to the bud and the bud neck and containing polarized actin cables were classified as partially polarized. Cells with more actin patches in the mother cell than in the bud were classified as depolarized. The confidence of the counts, which were done twice, was within  $\pm 3\%$ .

The polarized localization of GFP-Cdc42 and GFP-Rho1 was assessed in ~60 small-budded cells (bud <1/3 mother cell length) and visually scored based on whether the GFP or immunofluorescence signal was concentrated over background levels in the bud or was delocalized along the mother/daughter cortex or diffusely in the cytoplasm.

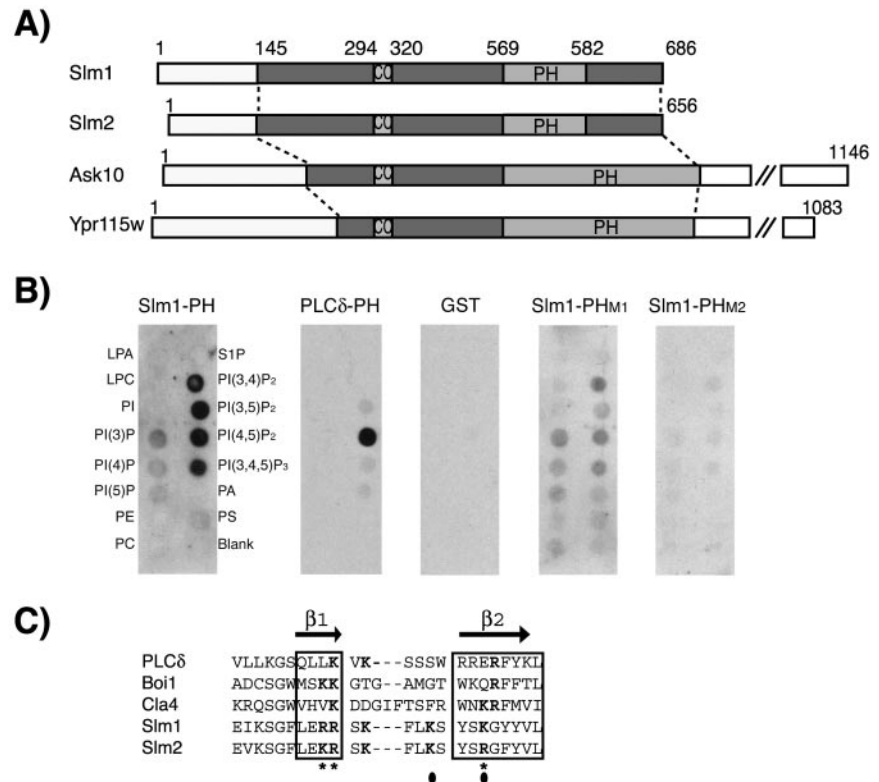
### In Vitro Pull-Down Assays

In vitro transcription and translation and labeling of proteins with [<sup>35</sup>S] Easy Tag Express Protein Labeling Mix (PerkinElmer Life and Analytical Sciences, Boston, MA) was performed using the rabbit T7 in vitro transcription/translation kit from Promega. *AVO2*, *BIT61*, or *YBR270C* cloned into vector TNT521 (Udan *et al.*, 2003) were used as DNA templates in the reactions. For pull-down assays, 6  $\mu$ l of product from in vitro transcription and translation reactions was incubated for 1 h at 4°C with 1  $\mu$ g of the different GST fusion proteins (or 6His-Slm1 and 6His-Slm2, purified as indicated above and bound to agarose beads) in binding buffer (20 mM Tris-HCl, pH 8.0, 150 mM NaCl, 1 mM EDTA, 0.1% Triton X-100, 0.1% Tween 20, and 0.1% SDS, containing protease inhibitors [1 mM PMSF, 1  $\mu$ g/ml leupeptin, and 1  $\mu$ g/ml pepstatin A]). Agarose beads then were collected by centrifugation in a microcentrifuge at 500  $\times$  g for 2 min and washed five times with 1 ml of cold binding buffer. Bound proteins were eluted and denatured in SDS sample buffer by incubation at 68°C for 15 min. Proteins were separated by standard 10% SDS-PAGE gels. Gels were dried and exposed to BiomaxMR film (Eastman Kodak, Rochester, NY).

### Coimmunoprecipitation Assays

*SLM1* and *SLM2* were expressed from the *GAL1* promoter as a fusion protein with a double HA epitope at the N terminus (pAS24, *CEN LEU2*) or as untagged proteins (pAS23, *CEN LEU2*). Cells were cultivated in selective raffinose medium to an A<sub>600</sub> of 0.5, followed by a 4- to 6-h galactose induction. To prepare whole cell extracts (typically from 2 liters of culture), yeast cells were resuspended in lysis buffer (50 mM Tris-HCl, pH 7.5, 50 mM NaCl, 0.1 mM EDTA, 0.1% NP-40, and 10% glycerol, and 1 mM PMSF, 1  $\mu$ g/ml leupeptin, and 1  $\mu$ g/ml pepstatin A), lysed with glass beads in a bead-beater

**Figure 1.** Domain organization of Slm1 and Slm2 and lipid binding specificity. (A) Schematic diagram of Slm1, Slm2, Ask10, and Ypr115w structures showing the locations of PH (PH) and coiled-coil (CC) domains, respectively. Light and dark shaded boxes indicate the regions conserved among all four proteins. (B) Nitrocellulose-immobilized phospholipids (PIP Strip) were incubated with recombinant fusion proteins of GST to the C terminus of Slm1 (amino acids 441–686) containing either the wild-type PH domain (Slm1-PH) or the mutant variants PH<sub>M1</sub> and PH<sub>M2</sub>. GST alone or a GST fusion to the PH domain of PLC $\delta$ , which specifically binds PtdIns(4,5)P<sub>2</sub> in vitro were used as controls. Bound proteins were visualized by Western blot analysis with anti-GST antibodies. Spots contained lysophosphatidic acid (LPA), lysophosphocholine (LPC), PtdIns(PI), PtdIns(3)P, PtdIns(4)P, PtdIns(5)P, phosphatidylethanolamine (PE), phosphatidylcholine (PC), sphingosine-1-phosphate (S1P), PtdIns(3,4)P<sub>2</sub>, PtdIns(3,5)P<sub>2</sub>, PtdIns(4,5)P<sub>2</sub>, PtdIns(3,4,5)P<sub>3</sub>, phosphatic acid (PA), and phosphatidylserine (PS). (C) Sequence alignment of the  $\beta$ 1/ $\beta$ 2 regions of Slm1 and Slm2 PH domains with related PH domains from PLC $\delta$ , Boi1, and Cla4. Secondary structure is indicated above the sequence alignment. Bold letters indicate residues required for interaction with phosphoinositide ligands. Asterisks and closed circles indicate amino acid residues targeted for mutagenesis in Slm<sub>M1</sub> and Slm<sub>M2</sub> PH domain mutants, respectively.



(6 × 30 s, 4°C; BioSpecs, Bartlesville, OK), and clarified by microcentrifugation (500 × *g*, 15 min, 4°C). TAP-tagged Avo2 or Bit61 was purified as described previously (Gould *et al.*, 2004) from 3 mg of whole cell extract (diluted 1:5 with lysis buffer), by using an IgG-Sepharose column followed by washing steps and cleavage with tobacco etch virus protease. The eluted protein was then applied to calmodulin-conjugated beads for the second purification step. After washing five times with lysis buffer containing 500 mM NaCl and 0.5% Triton X-100 and once with phosphate-buffered saline (PBS), the purified complexes were resuspended in 1 × SDS-PAGE sample buffer, denatured at 60°C for 10 min, and analyzed by SDS-PAGE and Western analysis by standard methods. To analyze Slm interaction with Tor2, a plasmid containing *HA-TOR2* (pAS25, *CEN*, *URA3 GAL1* containing 2 × *HA-TOR2*) (Kunz *et al.*, 2000) was introduced into strain W303a, and expression of *HA-TOR2* was induced by growing exponential yeast cultures for 4–6 h in the presence of 2% galactose. Yeast cell extracts (1 mg total protein diluted 1:5 in lysis buffer) were generated as described above and incubated with 1  $\mu$ g of purified recombinant 6His-Slm1 and 6His-Slm2 bound to Ni<sup>2+</sup>-agarose beads or beads alone for 1 h at 4°C. Beads were then collected by centrifugation (500 × *g*), and washed four times with lysis buffer and once with PBS. The purified complexes were resuspended in 1 × SDS-PAGE sample buffer, denatured at 60°C for 10 min, and analyzed by SDS-PAGE and Western analysis.

#### Alkaline Phosphatase Treatment of Protein Extracts and In Vitro Kinase Assays

Twenty-five micrograms of whole yeast cell extract lacking or containing phosphatase inhibitor cocktails I and II (Novagen, Madison, WI) were incubated with 1 U of alkaline phosphatase (ALP) (Roche Diagnostics, Indianapolis, IN) in the presence of 2 mM MgCl<sub>2</sub> for 30 min at 37°C. Samples were denatured at 60°C for 5 min and subjected to SDS-PAGE and Western analysis. In vitro protein kinase assays were performed as described previously (Inagaki *et al.*, 1999) by using 1  $\mu$ g of recombinant 6His-Slm1 and 6His-Slm2 and immunoprecipitated HA-Tor2 or HA-Tor2KD isolated from 0.5 mg of cell extract derived from W303a cells expressing *HA-TOR2* or *HA-TOR2KD*.

## RESULTS

### Slm1 and Slm2 Are Related Proteins Containing PH Domains

To identify novel PtdIns(4,5)P<sub>2</sub> effectors, we searched for yeast proteins that contain a PH domain. Thirty proteins

predicted to contain a total of 33 PH domains were identified in the yeast genome by using the program SMART (<http://www.smart.heidelberg.de>). Among these were known effectors of PtdIns(4,5)P<sub>2</sub> (Rom2, Boi1, Boi2, Num1, and Pld1; Farkasovsky and Kuntzel, 1995; Audhya and Emr, 2002; Hallett *et al.*, 2002; Sciorra *et al.*, 2002) and of PtdIns(4)P (the oxysterol-binding proteins Osh1 and Osh2 and the serine/threonine protein kinase Cla4; Levine and Munro, 2001; Levine and Munro, 2002; Roy and Levine, 2004; Wild *et al.*, 2004). The remaining 21 PH domain-containing proteins listed in the SMART database had not been reported previously to bind phosphoinositides. Among these were a group of 10 proteins with unknown functions. In this study, we explored the functions and regulation by phosphoinositides of two of these proteins, encoded by ORFs *YIL105C* and *YNL047C*. Because *YIL105C* and *YNL047C* exhibit synthetic genetic interaction with *MSS4* (see below), these genes were termed *SLM1* and *SLM2*.

Slm1 (686 amino acids, *YIL105C*) and Slm2 (656 amino acids, *YNL047C*) are highly related and share an overall amino acid sequence identity of 59% (Figure 1A). Slm1 and Slm2 also exhibit lower sequence homology (38% identity) within their central regions to two other yeast proteins: Ask10, a component of the RNA polymerase II complex that is involved in the cellular response to heat and oxidative stress (Page *et al.*, 1996; Cohen *et al.*, 2003), and a protein of unknown function encoded by ORF *YPR115W* (Figure 1B). Sequences related to Slm1 and Slm2 are conserved throughout the fungal kingdom, but no clear homologues are present in higher eukaryotes.

Slm1, Slm2, Ask10, and Ypr115w are all predicted to contain C-terminal PH domains (Figure 1A). However, unlike the Slm PH domains, the PH domains of Ask10 and Ypr115w are interrupted by several, up to 70 amino acid-

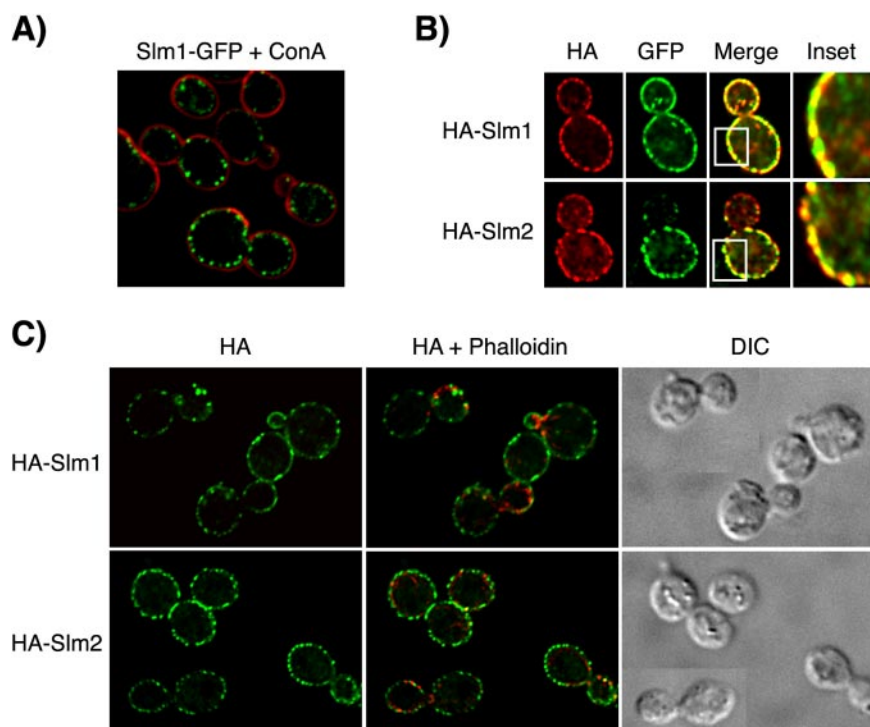


**Figure 2.** Slm1 and Slm2 localize to the plasma membrane. (A) Cells containing chromosomally expressed Slm1-GFP fusion protein were mounted on glass slides and the localization of the GFP fusion protein (shown in green) was visualized by fluorescence microscopy, whereas cell walls were visualized by staining with Alexa-594-conjugated concanavalin A (ConA, shown in red). (B) HA-Slm1 and HA-Slm2 are concentrated in clusters along the plasma membrane that contain Pma1-GFP. HA-Slm1 (top, red), HA-Slm2 (bottom, red) expressed from the *GAL1* promoter and chromosomally expressed Pma1-GFP (green) were visualized using antibodies directed against HA and GFP, respectively, followed by appropriate fluorescently labeled IgG. Yellow indicates signal overlap. The inset shows a magnification of the staining. (C) HA-Slm1 and HA-Slm2 do not localize to cortical actin patches. HA-Slm proteins were visualized as in B, whereas actin was stained with Alexa-594-conjugated phalloidin (shown in red). Differential interference images of the same cells are shown to the right.

long insertions, indicating that they may bind different ligands. Indeed, Ask10 is localized to the nucleus rather than to a membrane compartment (Cohen *et al.*, 2003). In addition to the PH domain, Slm1, Slm2, Ask10, and Ypr115w also contain a coiled-coil domain (Figure 1A). Coiled-coils are known to mediate protein-protein interactions and often promote homo- or heterodimerization. Thus, Slm1 and Slm2 are members of a novel protein family and have the potential to interact with both lipid and protein ligands.

#### *The Slm1 PH Domain Is a Polyphosphoinositide Binding Module*

To assess the lipid-binding activity of the Slm1 and Slm2 PH domains, we used a lipid overlay assay (Dowler *et al.*, 2002). This assay has been used extensively to characterize the lipid binding specificity of proteins. A GST fusion protein containing the PH domain of Slm1 was used to probe a panel of lipids spotted onto nitrocellulose membranes (PIP Strip; Echelon Biosciences). This qualitative assay showed that the Slm1 PH domain bound strongly to all multiply phosphorylated phosphoinositides tested, including PtdIns(3,4)P<sub>2</sub>, PtdIns(3,5)P<sub>2</sub>, PtdIns(4,5)P<sub>2</sub>, and PtdIns(3,4,5)P<sub>3</sub> (Figure 1B). The Slm1 PH domain also bound weakly to monophosphorylated forms of PI such as PtdIns(3)P, PtdIns(4)P, and PtdIns(5)P (Figure 1B). This contrasts with the highly specific lipid binding activity exhibited by the PH domain of PLC $\delta$ , which was tested as a control and exclusively bound to PtdIns(4,5)P<sub>2</sub> (Figure 1B). As expected, GST alone showed no detectable binding (Figure 1B). We conclude that the PH domain of Slm1 is a functional phosphoinositide-binding domain that binds promiscuously to polyphosphoinositides *in vitro*.

Structural studies of PH domains have shown that phospholipid binding in all PH domains examined so far is dependent on conserved basic residues located in a region spanning  $\beta$  strands 1 and 2 (Ferguson *et al.*, 1995, 2000; Figure 1C). An alignment of the Slm1 and Slm2 PH domains

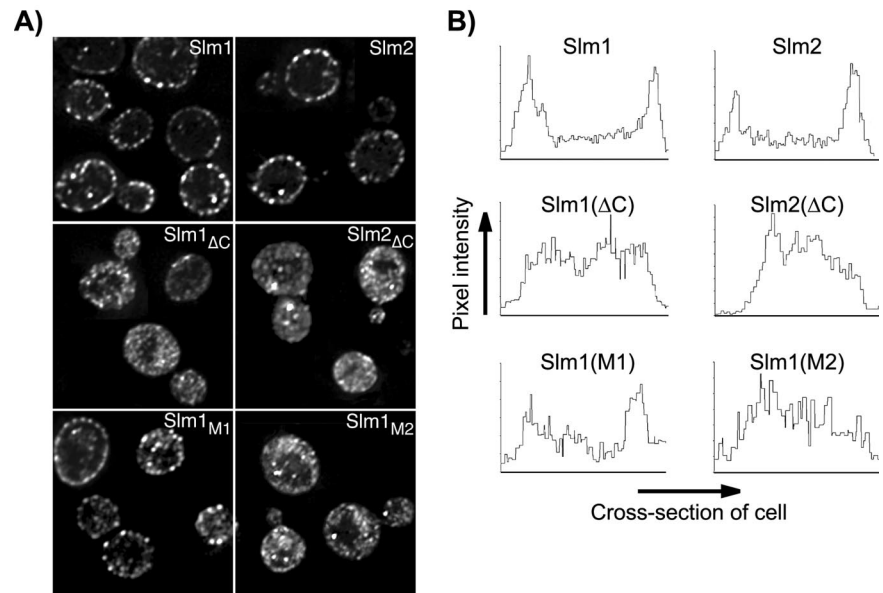
with a number of other PH domains showed that Slm1 and Slm2 contain basic residues in analogous positions (Figure 1C). Based upon this alignment, we constructed a panel of mutants in which several of these basic residues in the Slm1 PH domain were mutated in various combinations to alanine. These mutant PH domains were then tested in lipid overlay assays alongside the wild-type PH domain. We found that two mutations, K483A/K487A (designated PH<sub>M1</sub>) and R477A/R478A/K487A (designated PH<sub>M2</sub>), significantly reduced phosphoinositide binding to ~20 and 5%, respectively, of wild-type levels. Thus, as in previously characterized PH domains, conserved basic residues in the Slm1 PH domain are required for lipid binding.

#### *Slm1 and Slm2 Localize to the Plasma Membrane*

Many PH domains mediate the recruitment of their host protein to cellular membranes. To determine whether the PH domains of Slm1 and Slm2 serve a similar function, we first analyzed the subcellular localization of Slm1 and Slm2. As shown in Figure 2A, a chromosomally expressed GFP fusion to the C terminus of Slm1 localized in a patch-like pattern around the cell periphery, suggesting that Slm1-GFP localizes to the plasma membrane. Weak diffuse GFP signal also was observed in the cytoplasm, indicating that a minor portion of Slm1-GFP is soluble. Similar to Slm1-GFP, a chromosomally expressed Slm2-GFP fusion protein was concentrated in clusters at the plasma membrane (our unpublished data), but produced a GFP signal of much lower intensity, possibly due to lower expression levels of Slm2 compared with Slm1 (Ghaemmaghami *et al.*, 2003; our unpublished observations).

To confirm that Slm1 and Slm2 localize to the plasma membrane, we performed double labeling experiments by using a yeast strain expressing plasmid-borne HA-Slm1 and HA-Slm2 in combination with a chromosomally encoded GFP fusion to Pma1, the plasma membrane H<sup>+</sup>-ATPase (Serrano *et al.*, 1986). HA-tagged Slm1 and Slm2 fusion pro-

**Figure 3.** The PH domain and phosphoinositide binding activity are necessary for plasma membrane association of Slm1 and Slm2. (A) Subcellular localization of HA-tagged wild-type and mutant variants of Slm1 and Slm2 expressed under the control of the *GAL1* promoter and visualized by indirect immunofluorescence using antibodies against the HA-tag followed by Cy2-conjugated secondary antibodies. Shown are single z-sections of W303a cells expressing wild-type HA-tagged Slm1 and Slm2 (Slm1 and Slm2); C-terminally truncation mutants lacking the PH domain (Slm1 $_{\Delta C}$  and Slm2 $_{\Delta C}$ ) and full-length Slm1 point mutants containing substitutions in the PH domain (Slm1 $_{M1}$  and Slm1 $_{M2}$ ). (B) Quantification of plasma membrane association of wild-type and mutant Slm1 and Slm2 variants. A density profile plot was generated using NIH Image 1.62. Pixel intensity was determined by a "raw average plot" of a cross section through the center of the cell from single confocal slices obtained from four to six cells.



teins expressed from a low-copy vector under the control of the *GAL1* promoter colocalized with the endogenous Slm1-GFP signal in double labeling experiments (our unpublished data) and thus accurately reflected the localization of the endogenous Slm proteins. In agreement with earlier findings, Pma1-GFP exhibited a characteristic punctate fluorescence pattern along the plasma membrane (Figure 2B) that was often more pronounced in the mother cell (Malinska *et al.*, 2003). The fluorescent patterns of HA-Slm1 and HA-Slm2 showed significant overlap with the Pma1-GFP signal (Figure 2B), demonstrating that Slm1 and Slm2 localize to the plasma membrane.

The Slm-containing patch-like clusters at the plasma membrane were reminiscent of cortical actin patches (Mulholland *et al.*, 1999). However, neither Slm1-GFP nor HA-Slm1 colocalized with actin in double-labeling experiments by using phalloidin to visualize actin filaments and anti-HA or anti-GFP antibodies, respectively, to detect Slm1 (Figure 2C). Thus, both endogenous and plasmid-borne Slm1 and Slm2 proteins localize to a plasma membrane subcompartment that contains Pma1 but that is distinct from actin patches.

#### The PH Domains of Slm1 and Slm2 Mediate Plasma Membrane Localization

To determine whether the PH domains are required for targeting of Slm proteins to the plasma membrane, we investigated the subcellular localization of HA-tagged Slm truncation mutants Slm1 $_{\Delta C}$  (containing amino acids 1–453) and Slm2 $_{\Delta C}$  (containing amino acids 1–442), in which the C-termini containing the PH domains were deleted. Neither Slm1 $_{\Delta C}$  nor Slm2 $_{\Delta C}$  localized to the plasma membrane. Rather, they were distributed diffusely throughout the cytosol and to cytosolic speckles (Figure 3, A and B) demonstrating that the C-terminal domains of Slm1 and Slm2 mediate plasma membrane localization.

A functional PH domain was necessary for Slm1 and Slm2 localization, because the ability of Slm proteins to associate with the plasma membrane *in vivo* correlated directly with their lipid-binding activity *in vitro*. Accordingly, membrane association was severely reduced in the Slm1 $_{M2}$  PH triple mutant, which had lost its lipid binding activity *in vitro*.

This mutant accumulated in the cytosol and within cytosolic speckles (Figure 3, A and B), and only a small portion of the protein remained associated with the plasma membrane. By contrast, the Slm1 $_{M1}$  mutant that still retained some lipid binding *in vitro* was only partially delocalized from the plasma membrane (Figure 3, A and B). Together, our data demonstrate that Slm1 and Slm2 targeting to the plasma membrane is dependent on their PH domains and phosphoinositide binding activity.

#### Subcellular Localization of Slm Proteins Is Dependent on PtdIns(4,5)P<sub>2</sub> Synthesis

The broad *in vitro* phosphoinositide binding specificity of the Slm1 PH domain raised the question of which lipid was recognized by Slm proteins *in vivo*. To assess the *in vivo* lipid binding specificity, we determined the consequences of manipulating specific phosphoinositide pools on Slm localization. To do this, we took advantage of a panel of yeast mutants defective in the lipid kinases responsible for the synthesis of the various phosphoinositide species in yeast.

Of the lipids bound by the Slm1 PH domain *in vitro*, yeast cells contain PtdIns(4,5)P<sub>2</sub> and PtdIns(3,5)P<sub>2</sub>, whereas PtdIns(3,4)P<sub>2</sub> and PtdIns(3,4,5)P<sub>3</sub> have so far not been detected (Desrivieres *et al.*, 1998; Gary *et al.*, 1998; Homma *et al.*, 1998; Odorizzi *et al.*, 1998). Given the *in vivo* localization of Slm proteins to the cell periphery, we first investigated whether their localization is dependent on PtdIns(4,5)P<sub>2</sub> synthesis at the plasma membrane mediated by Mss4. Because *MSS4* is essential for growth, HA-Slm1 was expressed in cells containing the temperature-sensitive *mss4-2ts* allele. This temperature-sensitive mutation reduces cellular PtdIns(4,5)P<sub>2</sub> levels by 90% at the nonpermissive temperature of 37°C (Desrivieres *et al.*, 1998). Incubation of *mss4-2ts* cells at the nonpermissive temperature for 2 h caused a significant decrease of HA-Slm1 signal at the plasma membrane, accompanied by a concomitant increase in cytoplasmic signal (Figure 4, A and B). Under the same conditions, inactivation of *MSS4* also led to the delocalization of a PtdIns(4,5)P<sub>2</sub>-specific GFP reporter protein containing the PH domain of PLC $\delta$ , indicating that cellular PtdIns(4,5)P<sub>2</sub> levels were indeed down-regulated (our unpublished data). HA-Slm1 was already present in the cytoplasm in *mss4-2*

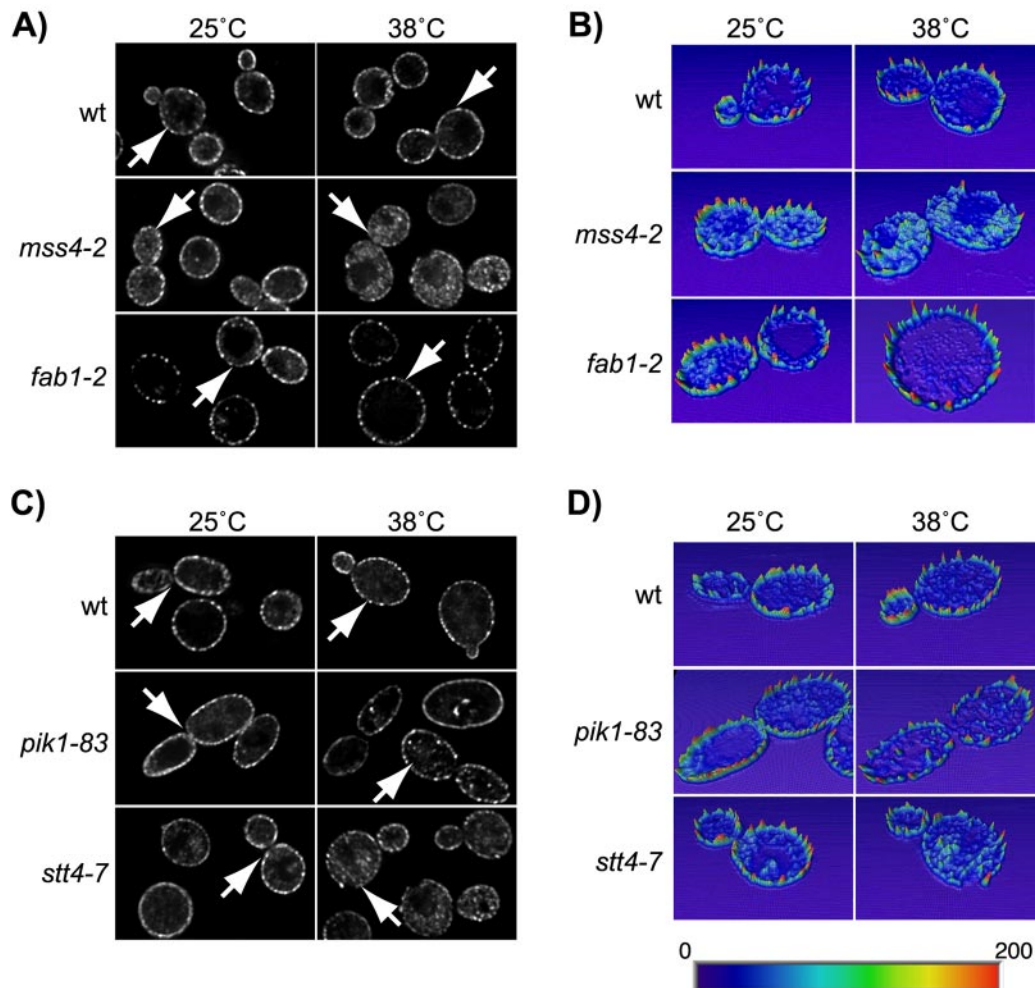


**Figure 4.** Localization of Slm1 is dependent on PtdIns(4,5)P<sub>2</sub> synthesis. The *YCp-HA-SLM1* plasmid was introduced into the wild-type strains JK9-3Da (A) and W303a (C), and into isogenic strains containing *mss4-2<sup>ts</sup>*, *fab1-2<sup>ts</sup>*, *pik1-83<sup>ts</sup>*, and *stt4-7<sup>ts</sup>* temperature-sensitive mutations. Indirect immunofluorescence was performed on cells grown at 25°C or shifted to 38°C for 1.5 h by using antibodies against the HA-tag followed by Cy2-conjugated secondary antibodies. (B and D) Quantification of pixel intensity. Heightfield visualizations were performed on single z-sections of representative cells (marked with arrows) by using Amira 3.0. Maximum pixel intensity is indicated in red; minimum pixel intensity in dark blue in the color scheme.

cells grown at the permissive temperature, whereas HA-Slm1 almost exclusively localized to the cell periphery in wild-type control cells grown at either 25 or 38°C (Figure 4, A and B). The increase in cytoplasmic HA-Slm1 in *mss4-2* cells reflected the redistribution of the protein from the plasma membrane into the cytoplasm and was not due to increased de novo synthesis of HA-Slm1, because HA-Slm1 similarly relocated into the cytosol in *mss4-2* cells that were shifted back to glucose medium to repress HA-Slm1 expression before incubation at nonpermissive temperature (our unpublished data). Based on these results, we conclude that Slm1 plasma membrane recruitment is at least in part dependent on PtdIns(4,5)P<sub>2</sub> synthesis.

The pool of PtdIns(4)P that serves as the substrate for Mss4 is generated by the essential PI 4-kinase Stt4, which also localizes primarily to the plasma membrane (Audhya and Emr, 2002). A separate pool of cellular PtdIns(4)P is generated on Golgi membranes by the second essential PI 4-kinase, Pik1 (Audhya *et al.*, 2000; Hama *et al.*, 1999). Inactivation of Pik1 by using the temperature-sensitive *pik1-83<sup>ts</sup>* allele (Audhya *et al.*, 2000) had little effect on the intracellular

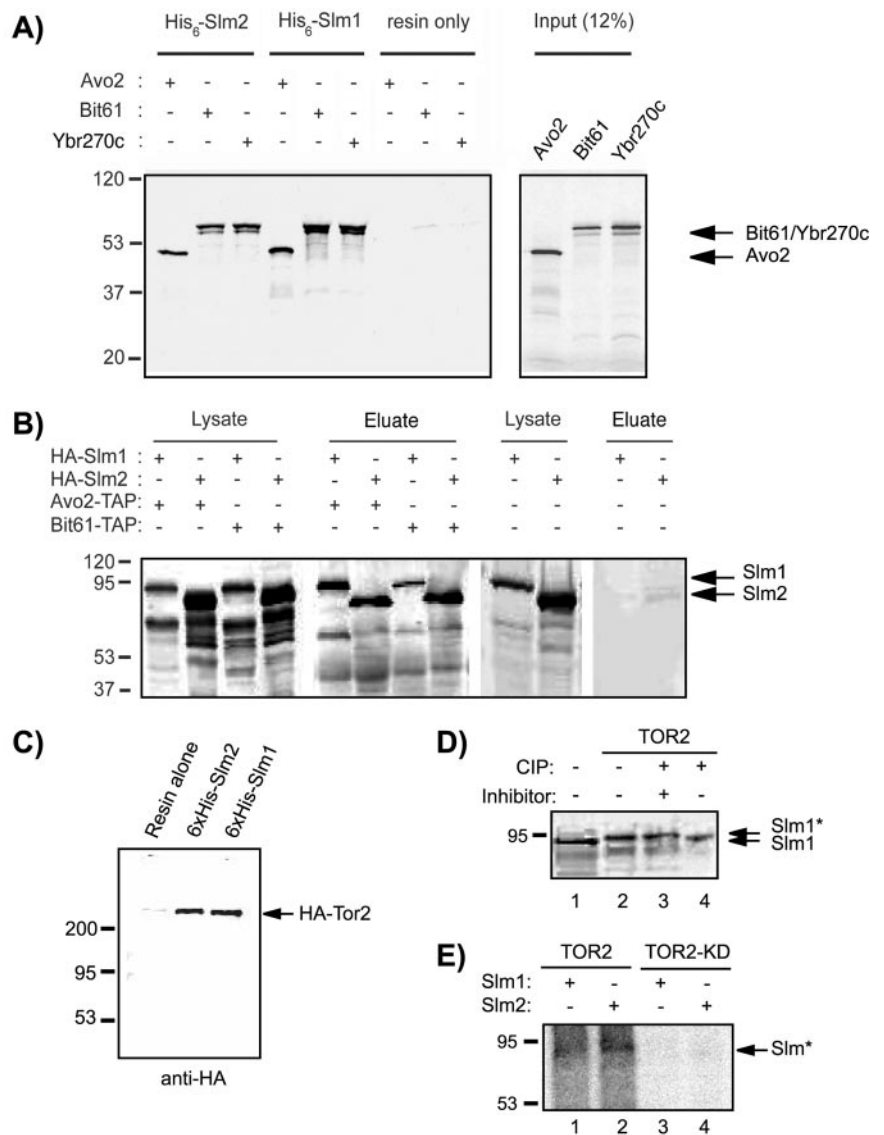
distribution of HA-Slm1 (Figure 5, C and D). In contrast, a portion of HA-Slm1 was redistributed from the cell surface into the cytosol and onto intracellular speckles (Figure 4, C and D) in the temperature-sensitive *stt4-7* mutant at 38°C (Muhua *et al.*, 1998). Therefore, it seems that the Stt4-dependent plasma membrane pool of PtdIns(4)P modulates plasma membrane localization of Slm1, most likely by serving as the precursor for PtdIns(4,5)P<sub>2</sub>.

Slm1 still localized to the plasma membrane in cells containing a temperature-sensitive mutation in *FAB1* (*fab1-2*) encoding the single, nonessential PtdIns(3)P 5-kinase (Yamamoto *et al.*, 1995; Gary *et al.*, 1998; Odorizzi *et al.*, 1998; Figure 4, A and B), thus demonstrating that Slm1 localization is independent on cellular PtdIns(3,5)P<sub>2</sub> levels.

Another approach to demonstrate that Slm1 subcellular targeting is dependent on PtdIns(4,5)P<sub>2</sub> is to manipulate cellular PtdIns(4,5)P<sub>2</sub> levels by expression of a lipid phosphatase. The *Salmonella* phosphatase SigD (also known as SopB) was previously shown to promote the disappearance of PtdIns(4,5)P<sub>2</sub> in mammalian cells and to displace PLCδ-PH-GFP from the plasma membrane (Terebiznik *et al.*, 2002).



**Figure 5.** Slm1 and Slm2 physically interact with Tor2 and TORC2 components. (A) In vitro-transcribed and -translated <sup>35</sup>S-labeled Avo2, Bit61, and Ybr270c were incubated with recombinant 6His-Slm1 and 6His-Slm2 fusion proteins bound to nickel beads or with resin alone. Bound <sup>35</sup>S-labeled proteins that remained after washing were analyzed by SDS-PAGE and autoradiography. The molecular masses of protein markers are indicated to the left. The inferred positions of Avo2, Bit61, and Ybr270c are indicated by arrows. (B) Western blot analysis of proteins associated with Tap-Avo2 and TAP-Bit61 during TAP purification experiments. Cell extracts were prepared from a strain that expressed C-terminally TAP-tagged Avo2 or Bit61 and contained HA-Slm1 or HA-Slm2 expressed under the control of the *GAL1* promoter and were then subjected to sequential purifications on IgG and calmodulin affinity resins. Bound proteins were eluted with SDS-PAGE buffer, separated on 10% SDS-PAGE gels, and immunoblotted with antibodies directed against HA. The inferred positions of HA-Slm1 and HA-Slm2 are indicated by arrows. (C) HA-Tor2 associate with Slm1 and Slm2. Clarified cell lysates from a wild-type strain expressing *HA-TOR2* were incubated with nickel beads lacking or containing bound 6His-Slm1 or 6His-Slm2. Bound proteins were subjected to SDS-PAGE analysis and Western blotting with HA monoclonal antibody (mAb). The inferred position of HA-Tor2 is indicated by an arrow. (D) Yeast cell extracts from strain JK9-3D transformed with vector alone (lane 1) or *HA-TOR2* (lanes 2-4) were incubated with alkaline phosphatase (CIP) in the presence (+) or absence (-) of phosphatase inhibitor cocktail as indicated, before SDS-PAGE analysis and Western blotting with HA mAb. The asterisk indicates the phosphorylated form. (E) Recombinant 6His-Slm1 (lanes 1 and 3) and 6His-Slm2 (lanes 2 and 4) were incubated with HA-Tor2 or HA-Tor2KD immunoprecipitated from cell lysates in the presence of [<sup>32</sup>P]ATP. After SDS-PAGE, <sup>32</sup>P-labeled proteins (denoted with an asterisk) were visualized by autoradiography.



To assess the effects of SigD expression on Slm1 targeting in yeast, we placed SigD under the control of the *GAL1* promoter and introduced it into cells containing chromosomally encoded Slm1-GFP. As expected, Slm1-GFP was localized in a punctate pattern along the plasma membrane in cells grown in glucose medium where SigD expression is repressed (Supplementary Figure 1). By contrast, in cells grown in galactose medium, which induces SigD expression, the Slm1-GFP signal in plasma membrane clusters decreased in intensity and clusters often were not evident anymore (Supplementary Figure 1). SigD expression efficiently lowered plasma membrane PtdIns(4,5)P<sub>2</sub> levels under these conditions, because it induced the detachment of the PLC $\delta$ -PH-GFP fusion protein from the membrane (our unpublished data). Together, these data demonstrate a requirement for PtdIns(4,5)P<sub>2</sub> in recruiting Slm1 and Slm2 to the plasma membrane.

#### *SLM1 and SLM2 Synthetically Interact with Mutations in STT4 and MSS4*

To further investigate a relationship between Slm1/2 and the Stt4/Mss4 pathway, we looked for synthetic enhance-

ment between mutations that enfeeble Stt4 or Mss4 activity and mutations in *SLMs*. Individual *slm1* $\Delta$  or *slm2* $\Delta$  deletion mutants conferred no growth defect. However, when the *slm1* $\Delta$  mutation was combined with the temperature-sensitive *stt4-7* mutation, *slm1* $\Delta$  *stt4-7* doubly mutant segregants were never recovered at the permissive temperature for *stt4-7* after sporulation and tetrad analysis ( $n = 53$ ; see *Materials and Methods*), indicating that the combination of these mutations is lethal. Likewise, when *slm1* $\Delta$  was combined with the *mss4-2* temperature-sensitive mutation by crossing strains JK503 and JK511 (*mss4::HIS3 ura3-52::mss4-2::URA3*), no meiotic progeny were obtained from dissected tetrads ( $n = 47$ ) that were Ura<sup>+</sup> His<sup>+</sup> G418<sup>R</sup>. Therefore, *slm1* $\Delta$  is synthetically lethal with *stt4-7* and *mss4-2*.

Although *slm2* $\Delta$  *stt4-7* and *slm2* $\Delta$  *mss4-2* doubly mutant segregants were obtained from dissected tetrads ( $n = 22$  and  $n = 32$ , respectively), they formed smaller colonies than the individual single mutants at 25°C and failed to grow at temperatures at or above 38°C (our unpublished data). Thus, *slm2* $\Delta$  confers synthetic growth defects when combined with *stt4* and *mss4* mutations. The much higher abundance of

Slm1 protein compared with Slm2 (Ghaemmaghami *et al.*, 2003; our unpublished observations) may explain why mutations in *SLM1* confer more severe growth defects than mutations in *SLM2*.

The synthetic lethality and synthetic sickness phenotypes observed between *slmΔ*, and mutations in *STT4* and *MSS4* suggest that these genes function in a common process. Together with our previous results these data are thus consistent with Slm proteins being effectors of PtdIns(4,5)P<sub>2</sub> and acting in the Stt4/Mss4 signaling pathway.

### *Slm1 and Slm2 Physically Interact with TORC2 Components*

Unlike the isolated Slm1 PH domain or the PtdIns(4,5)P<sub>2</sub>-binding PLCδ-PH-GFP fusion protein, which localize uniformly along the plasma membrane (Yu *et al.*, 2004), Slm1 and Slm2 target to distinctive plasma membrane clusters. This suggests that Slm subcellular targeting also is dictated by a PtdIns(4,5)P<sub>2</sub>-independent component and may involve protein-protein interaction(s). Recent genome-wide two-hybrid screens identified several candidate Slm1 or Slm2 interacting proteins (Uetz *et al.*, 2000; Ito *et al.*, 2001). Among these, Avo2 and Ybr270c interact with both Slm proteins (Uetz *et al.*, 2000; Ito *et al.*, 2001). Avo2 associates with the phosphatidylinositol kinase-related protein kinase Tor2 as part of the TORC2 signaling complex (Abraham, 2002; Loewith *et al.*, 2002; Wedaman *et al.*, 2003), one of two distinct protein complexes containing Tor2 (Crespo and Hall, 2002). TORC2 is composed of Tor2, Avo1, Avo2, Avo3, Lst8, and Bit61 (Loewith *et al.*, 2002; Wedaman *et al.*, 2003; Reinke *et al.*, 2004) and mediates the essential Tor2-unique function required for the regulation of cell cycle-dependent actin polarization (Crespo and Hall, 2002). Ybr270c is highly related (45% amino acid identity and 61% similarity) to Bit61, and both proteins have been isolated in two-hybrid screens as binding partners of the TORC2 component Avo3 (Ito *et al.*, 2001; Uetz *et al.*, 2000). Notably, similar to Slm proteins, Tor2 and TORC2 components have been shown to localize to punctate clusters at or near the plasma membrane (Kunz *et al.*, 2000; Wedaman *et al.*, 2003). Together, these findings suggest that Slm1 and Slm2 are novel components of the TORC2 complex.

To confirm the physical association of Slm proteins with Avo2, Bit61, and Ybr270c, we performed *in vitro* pull-down assays. Avo2, Bit61, and Ybr270c were radioactively labeled using *in vitro* transcription/translation reactions in the presence of [<sup>35</sup>S]methionine and then incubated with recombinant purified 6His-Slm1 and 6His-Slm2 protein bound to agarose beads. After washing, the proteins retained on the beads were visualized by autoradiography. We found that beads containing 6His-Slm1 fusion protein, but not resin alone, efficiently and specifically retained Avo2, Bit61, and Ybr270c (Figure 5A). All three proteins also were precipitated on beads containing bound 6His-Slm2 (Figure 5A). We thus conclude that Slm1 and Slm2 bind Avo2, Bit61, and Ybr270c *in vitro*.

We next used the tandem affinity purification (TAP) method (Gould *et al.*, 2004) to test whether Slm1 and Slm2 interact with Avo2 and Bit61 *in vivo*. We focused on Avo2 and Bit61, because these proteins had been previously characterized. Cell extracts of yeast cells containing chromosomally expressed TAP-tagged Avo2 or Bit61 and expressing plasmid-borne HA-Slm1 or HA-Slm2 were subjected to successive affinity purification on IgG-Sepharose (first step) and calmodulin-agarose (second step). The affinity-purified Avo2-TAP and Bit61-TAP complexes were then separated by SDS-PAGE and analyzed by Western blot analysis by

using anti-HA antibodies to detect copurified HA-tagged Slm1 or Slm2.

Prominent bands of ~70 kDa that correspond well with the predicted molecular masses of HA-Slm1 (78 kDa) and HA-Slm2 (75 kDa) were recovered from extracts containing HA-tagged Slm proteins in the Avo2-TAP and Bit61-TAP purification experiments, but they were absent from extracts containing untagged Slm1 or Slm2 proteins (Figure 5B). These 70-kDa protein bands also were not recovered in control experiments by using whole cell extracts from a yeast strain that expresses HA-Slm1 or HA-Slm2 but contains untagged Avo2 or Bit61 (Figure 5B). Thus, HA-Slm1 and HA-Slm2 are copurified only in the presence of Avo2-TAP or Bit61-TAP. We conclude that Slm1 and Slm2 specifically interact with both Avo2 and Bit61 *in vitro* and *in vivo*.

To further assess whether Slm1 and Slm2 are part of the TORC2 complex, we tested whether Slm1 and Slm2 also could be copurified with Tor2. Perhaps due to instability of the TORC2 complex, we were unable to demonstrate copurification of HA-tagged Tor2 with chromosomally expressed Slm1 and Slm2 TAP fusion proteins during TAP affinity purification. However, when purified recombinant 6His-tagged Slm1 and Slm2 proteins, immobilized on agarose beads, were incubated with whole yeast cell extracts containing HA-Tor2, a protein with the predicted molecular mass of Tor2 of ~280 kDa was specifically retained on Slm1- and Slm2-containing beads, but not on resin alone (Figure 5C). Together, these results demonstrate that Slm1 and Slm2 physically associate with Tor2 and TORC2 components in a protein complex.

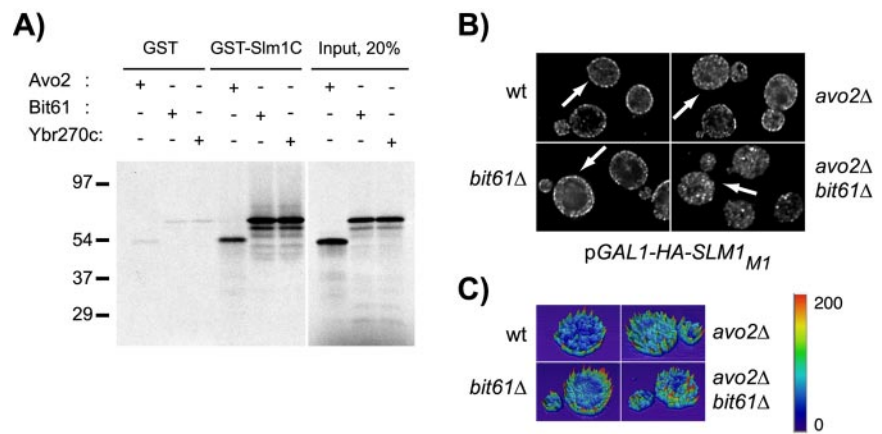
In the course of these experiments, we noticed an apparent shift of the Slm1-TAP (Figure 5D, lanes 2 and 3) and Slm2-TAP (our unpublished data) fusion proteins to a higher molecular mass when HA-TOR2 was overexpressed in these cells. This upshift in molecular mass likely reflects phosphorylation of Slm, because phosphatase treatment reverted the effect (Figure 5D, lane 4). Phosphorylation is either directly mediated by Tor2 or a Tor2-regulated protein kinase associated with TORC2, because recombinant 6His-Slm1 and -Slm2 proteins could be radioactively labeled in *in vitro* kinase assays in the presence of [<sup>γ</sup>-<sup>32</sup>P]ATP and immunoprecipitates containing HA-Tor2 (Figure 5E). In contrast, no phosphorylation was observed in kinase assays containing HA-Tor2 kinase-dead (Tor2KD) immunoprecipitates (Figure 5E). Thus, the TORC2 complex may regulate Slm function through phosphorylation.

### *Interaction with Bit61 and Avo2 Stabilizes Slm1 at the Plasma Membrane*

Because Slm1 and Slm2 physically interact with TORC2, we wanted to investigate its effect on Slm association with the plasma membrane. Our previous localization studies showed that the Slm1 deletion mutant Slm1<sub>ΔC</sub>, which contains amino acids 1–453 of Slm1, but lacks the C-terminal 233 amino acids that include the PH domain, was predominantly cytosolic. In contrast, a significant portion of Slm1 reproducibly remained associated with the plasma membrane when cellular PtdIns(4,5)P<sub>2</sub> levels were down-regulated in the *mss4-2* mutant. This suggested that the Slm C-terminus not only binds PtdIns(4,5)P<sub>2</sub> but also mediates protein-protein interaction, potentially with TORC2 and that these interactions contribute to Slm localization. To test this, we performed pull-down assays with a GST fusion protein containing the Slm1 C-terminal domain (GST-Slm1C comprising amino acids 441–686 of Slm1) and <sup>35</sup>S-labeled Avo2, Bit61, and Ybr270c proteins, generated by *in vitro* transcription/translation reactions. We found that all three proteins

**Figure 6.** Interaction with TORC2 stabilizes Slm1 association with the plasma membrane.

(A) The Slm1 C terminus can mediate interaction with TORC2 components. In vitro-transcribed and -translated <sup>35</sup>S-labeled Avo2, Bit61, and Ybr270c were incubated with resin alone or with resin containing GST fused in-frame to the Slm1 C terminus (GST-Slm1C; containing amino acids 441–686 of Slm1). Bound <sup>35</sup>S-labeled proteins that remained after washing were analyzed by SDS-PAGE and autoradiography. The molecular masses of protein markers are indicated to the left. (B) Plasmid pJK702 (*GAL1-HA-SLM1*) was introduced into wild-type cells (W303a), and isogenic *avo2Δ*, *bit61Δ*, *ybr270cΔ* single mutant, or *avo2Δ bit61Δ* double mutant cells. Cells were grown to early exponential phase in raffinose medium at 25°C and HA-Slm1 expression was induced by addition of galactose and further incubation for 2 h. HA-Slm1 was visualized in fixed cells as described in Figure 3. (C) Heightfield visualizations were performed on single z-sections of representative cells (marked with arrows) by using Amira 3.0. Maximum pixel intensity is indicated in red; minimum pixel intensity in dark blue in the color scheme.



efficiently bound to GST-Slm1C, but not to GST alone (Figure 6A). Thus, the Slm1 C terminus contains binding sites for PtdIns(4,5)P<sub>2</sub> and TORC2.

To determine whether TORC2 interaction is required for stabilizing Slm1 at the plasma membrane, we investigated whether the localization of the Slm1<sub>M1</sub> mutant, which has reduced PtdIns(4,5)P<sub>2</sub> binding activity, was affected in yeast cells lacking individual TORC2 components. HA-Slm1<sub>M1</sub> localized predominantly to the plasma membrane in wild-type cells but became more cytosolic in yeast cells containing single deletion mutants in *AVO2*, *BIT61*, or *YBR270C* (Figure 6, B and C; our unpublished data). These effects were additive, as HA-Slm1<sub>M1</sub> became significantly more delocalized from the plasma membrane in *avo2Δ bit61Δ* double mutant cells as compared with the single mutants (Figure 6, B and C). Thus, the presence or absence of TORC2 components that physically interact with Slm1 influences Slm1 association with the plasma membrane. Together, our data suggest that Slm localization is coordinately regulated by binding to PtdIns(4,5)P<sub>2</sub> and TORC2.

#### *Slm1 and Slm2 Have Redundant Functions and Are Essential for Growth*

To examine the phenotypic effects associated with loss of SLM function, we constructed a diploid yeast strain heterozygous for deletion alleles of *SLM1* and *SLM2*. Sporulation and tetrad analysis revealed that deletion of both genes led to inviability (Figure 7A). Microscopic examination of doubly mutant spores showed that the spores germinated, but arrested growth in various stages of the cell cycle within one generation (our unpublished data). Slm function is therefore required for cell growth after spore germination. Conditional expression of wild-type *SLM1* (Figure 7B) or *SLM2* (our unpublished data) from the *GAL1* promoter restored growth to *slm1Δ slm2Δ* double mutant cells on medium containing galactose as the carbon source, demonstrating that the lethality of double mutant cells is due to loss of Slm functions. Together, these data demonstrate that Slm1 and Slm2 are functionally redundant and perform an essential function required for cell growth.

To confirm a role of PtdIns(4,5)P<sub>2</sub> in the regulation of Slm activity, we next asked whether up-regulation of cellular PtdIns(4,5)P<sub>2</sub> levels could suppress the lethality of *slmΔ* mutant cells. Yeast cells lacking the nonessential

PtdIns(4,5)P<sub>2</sub> 5-phosphatase *INP51* have a two- to fourfold increase in cellular levels of PtdIns(4,5)P<sub>2</sub> (Stolz *et al.*, 1998a,b). We found that disruption of the *INP51* gene in a *slmΔ* null mutant strain containing the glucose-repressible *SLM1* gene was able to suppress the lethality of this strain on glucose medium (Figure 7B). This result suggests that PtdIns(4,5)P<sub>2</sub> positively regulates Slm function and likely activates the residual Slm1 protein that is present in these cells due to leaky expression from the *GAL1* promoter. In addition, this result implicates Inp51 as a negative regulator of the Slm pathway.

#### *PtdIns(4,5)<sub>2</sub> Binding Is Essential for Slm In Vivo Function*

We next wanted to determine whether the lipid binding activity of Slm1 and Slm2 is important for their function in vivo. We used a plasmid shuffle assay to assess the ability of Slm mutants lacking a functional PH domain to provide Slm function in vivo. *slm1Δ slm2Δ* double mutant cells carrying a *SLM2 URA3* plasmid were transformed with a second plasmid containing *LEU2* as a marker and expressing either wild-type *SLM1*, or the mutant versions *SLM1<sub>ΔC</sub>* and *SLM1<sub>M2</sub>*. Transformants were then streaked on solid medium containing 5-fluoroorotic acid (5-FOA) to counterselect the *SLM2 URA3* plasmid. We found that the lethality of *slm* doubly mutant cells was complemented on 5-FOA-containing medium only by wild-type *SLM1*, but not by the C-terminal truncation mutant *SLM1<sub>ΔC</sub>* or the *SLM1<sub>M2</sub>* mutant, which is defective for phosphoinositide binding (Figure 7C). We thus conclude that Slm function is dependent on an intact PH domain that can bind PtdIns(4,5)P<sub>2</sub>.

#### *Slm Proteins Are Required for Polarized Actin Assembly*

The TORC2 signaling complex and the Stt4/Mss4 pathway have both been linked to the regulation of actin cytoskeleton polarization (Desrivieres *et al.*, 1998; Homma *et al.*, 1998). To determine whether Slm proteins, like Tor2, Stt4, and Mss4, are required for proper actin organization, we examined the actin cytoskeleton in cells containing the temperature-sensitive *slm1-3* allele (*slm1-3 slm2Δ*; strain JK515). The *slm1-3* allele was generated in the course of our mutational analysis of PH domain residues and contains two point mutations in the PH domain (K501A, R505A) that reduce PtdIns(4,5)P<sub>2</sub> binding activity by ~50% (our unpublished data). This enfeeblled Slm1 mutant is able to support growth at 26°C, but

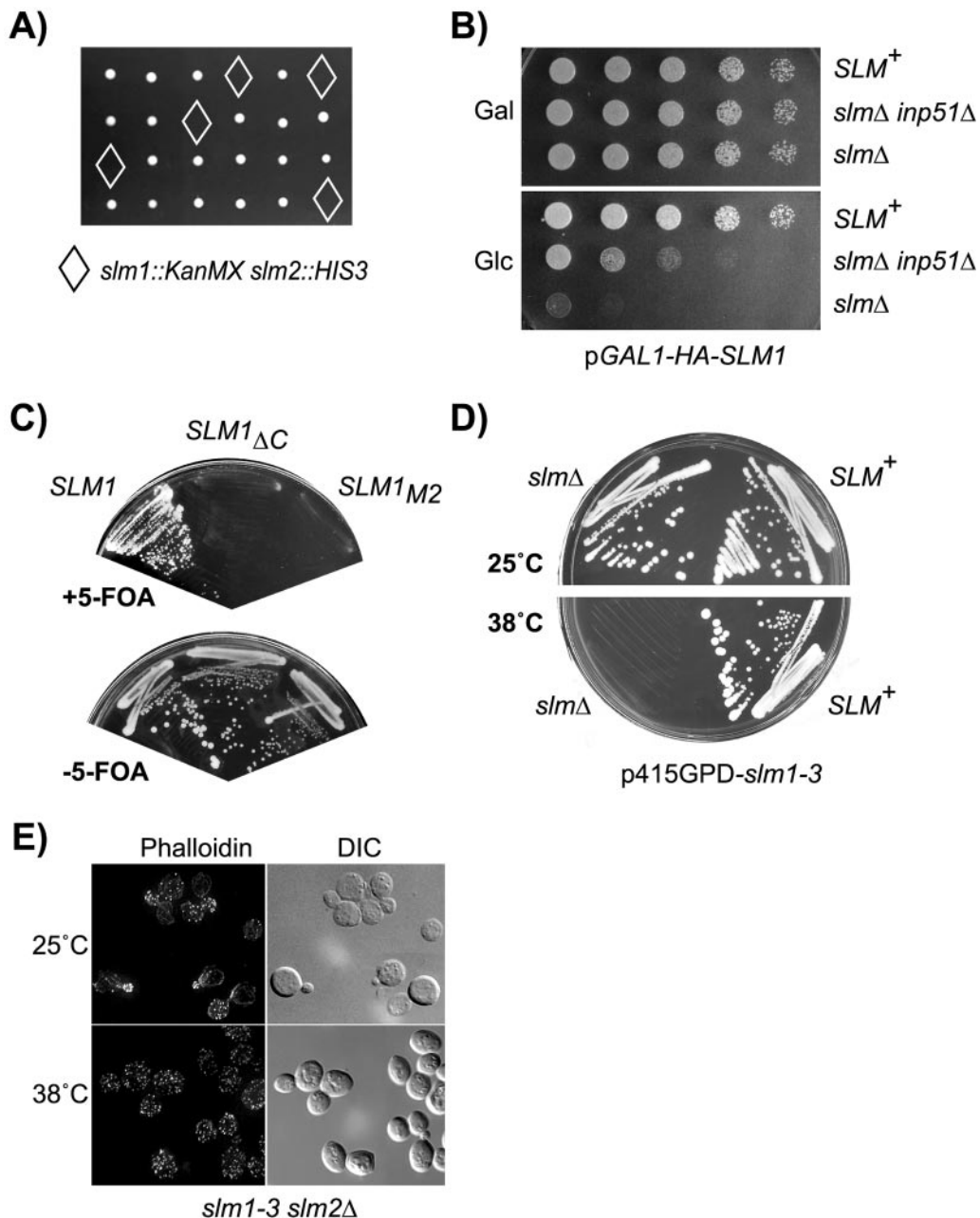


**Figure 7.** Slm1 and Slm2 are essential for growth and actin cytoskeleton polarization. (A) Viable meiotic progeny of the *SLM1/slm1::KanMX SLM2/slm2::HIS3* heterozygous diploid strain JK507 were recovered after microdissection of spores on YPD plates that were either G418-resistant (indicative of *slm1::KanMX*) or histidine prototroph (indicative of *slm2::HIS3*), but not both (marked by diamonds). (B) The lethality of *slm* null mutants is suppressed by conditional expression of *SLM1* or by disruption of *INP51*. Serial dilutions of cultures of wild-type (W303a) or of *slm1-3 slm2Δ* (JK516) and *slm1-3 slm2Δ inp51Δ* (JK518) mutant cells containing galactose-inducible *SLM1* (*pGAL1-HA-SLM1*) were spotted onto rich medium containing glucose (Glc) or galactose (Gal) as carbon source. Shown are plates incubated for 3 d. (C) Only a *LEU2* plasmid containing wild-type *SLM1* but not the *SLM1<sub>ΔC</sub>* and *SLM1<sub>M2</sub>* mutant variants can support growth of strain JK513 (*slm1::KanMX slm2::HIS3 YCpURA3Gal1-HA-SLM2*) on medium containing 5-fluoroorotic acid (+5-FOA), which counterselects the *SLM2 URA3* plasmid. (D) Wild-type and *slm1-3 slm2Δ* mutant cells were streaked on solid SD-Ura medium and incubated at 25 or 38°C for 3 d. (E) Loss of Slm function causes actin cytoskeletal defects. Exponentially growing *slm1-3 slm2Δ* yeast cells were grown at 25°C or shifted to 38°C for 2 h. Cells were fixed and stained with Alexa-594-phalloidin to visualize the actin cytoskeleton.

not at temperatures  $\geq 38^\circ\text{C}$  (Figure 7D) when expressed from a low-copy vector in *slm1Δ slm2Δ* double mutant cells.

Incubation of *slm1-3 slm2Δ* cells at 38°C for 2 h resulted in severe cytoskeletal defects. More than 80–90% of small- to medium-budded cells displayed cortical actin patches that were distributed randomly between mother and daughter

cell, rather than being concentrated in the emerging bud (Figure 7E). Furthermore, actin cables were either faint or completely absent. In contrast, the actin cytoskeleton in *slm1-3 slm2Δ* cells grown at the permissive temperature was similar to wild-type cells, with actin cables traversing from mother to bud and actin patches polarized toward the bud

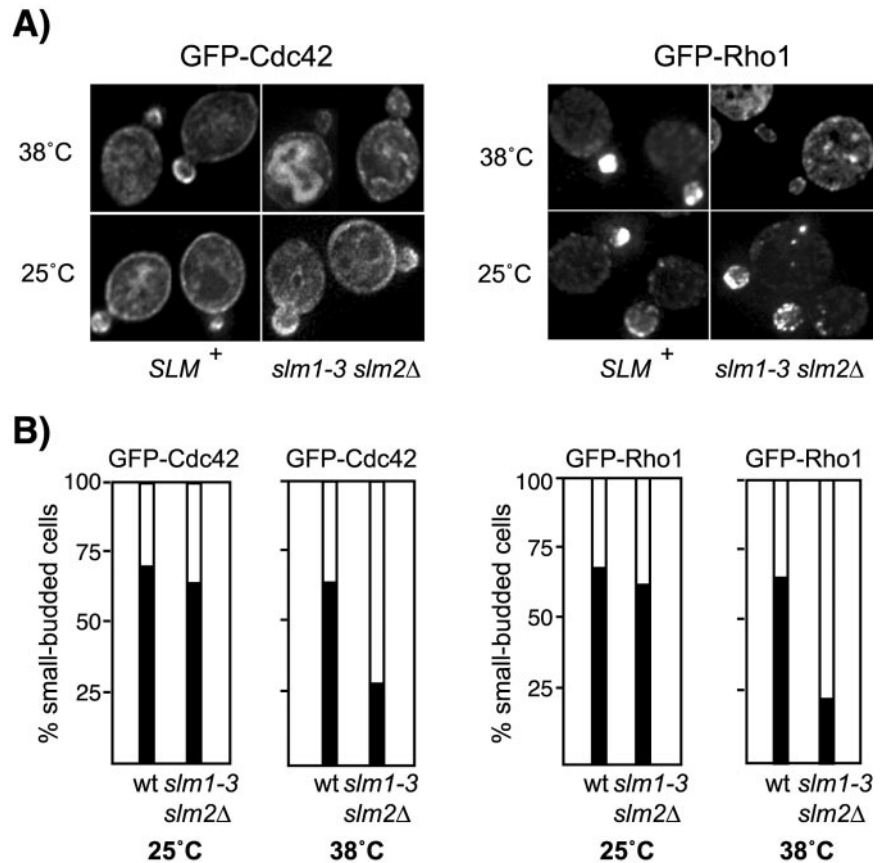


**Figure 8.** Polarized localization of Cdc42 and Rho1 is perturbed in *slmΔ* mutant cells. (A) The distribution of GFP-Rho1 and GFP-Cdc42 in wild-type and *slm1-3 slm2Δ* mutant cells is shown. Exponential cultures were grown in selective medium at 25°C followed by growth at 38°C for additional 2 h. Expression of GFP-Cdc42 was induced on SD-Leu-Met medium for 1 h at 25°C before shift to nonpermissive temperature. GFP-Cdc42 and GFP-Rho1 localization was visualized by immunofluorescence in living cells mounted in 1% agarose. (B) Approximately 60 small-budded cells expressing GFP-Cdc42 and GFP-Rho1 were scored for polarized distribution of the GFP signal to the bud (black bars) or depolarized localization to the cortex or the cytoplasm (white bars).

tip (Figure 7E). The actin and growth phenotypes of *slm1-3 slm2Δ* mutants were reversible after shorter periods of incubation (4–6 h) at 38°C (our unpublished data). However, after overnight incubation at the nonpermissive temperature, ghost cells indicative of dead or lysed cells accumulated, and cells had morphological defects, including aberrations in cell shape and size. In addition, these cells often grew as chains of cells suggesting defects in cell separation (our unpublished data). Together, our data suggest that Slm1 and Slm2 play redundant roles required for cell growth and for the proper assembly of a polarized actin cytoskeleton.

#### The Polarized Distribution of Cdc42 and Rho1 Is Perturbed in *slm* Mutant Cells

The two Rho GTPases Cdc42 and Rho1 both depend on actin cables to concentrate at sites of polarized growth, such as the growing bud (Abe *et al.*, 2003; Wedlich-Soldner *et al.*, 2003; Pruyne *et al.*, 2004). To confirm that actin cable assembly and polarization is defective in *slm* mutant cells, we examined the localization of GFP-Cdc42 and GFP-Rho1 fusion proteins in wild-type and *slm1-3 slm2Δ* mutant cells. As reported previously (Richman *et al.*, 2002), GFP-Cdc42 localized to the plasma membrane and internal membranes and was clustered at the presumptive bud site and in small buds in wild-type and *slm1-3 slm2Δ* cells grown at 25°C (Figure 8, A and B). GFP-Rho1 also was polarized and localized almost exclusively in the growing bud under these conditions (Figure 8, A and B). After 2 h at 38°C, the fraction of *slm1-3 slm2Δ* cells that retained the polarized distribution of GFP-Cdc42 and GFP-Rho1 was significantly reduced, whereas it remained relatively constant in wild-type cells (Figure 8, A and B). Because the retention of Cdc42 and Rho1 at the bud

requires actin cables, our results thus support a role of Slm proteins in actin cable organization.

#### PKC1 Is a Dosage Suppressor of *slm* Null Mutants

Previous genetic studies suggested that TORC2 acts upstream or in coordination with the Stt4/Mss4 pathway to control actin polarization through the cell integrity pathway (Schmidt *et al.*, 1997; Helliwell *et al.*, 1998a,b; Loewith *et al.*, 2002). Accordingly, genes encoding Mss4 or components of the cell integrity pathway, including the GTP exchange factor Rom2; the partially redundant GTPases Rho1 and Rho2; Pkc1; and a mitogen-activated protein kinase (MAPK) cascade module, including Bck1, the redundant Mkk1 and Mkk2, and Mpk1, act as high-copy suppressors of *tor2ts* or TORC2 mutants (Schmidt *et al.*, 1997; Helliwell *et al.*, 1998a,b; Loewith *et al.*, 2002). To test whether Slm1 and Slm2 control cell growth and actin polarization through the cell integrity pathway, we examined whether overexpression of cell integrity pathway components can suppress the phenotypes of *slmΔ* null mutants. We found that only overexpression of *PKC1* suppressed the lethality of Slm-depleted cells on glucose (Figure 9A) or of *slm1-3 slm2Δ* cells at 38°C (our unpublished data). Plasmid shuffling experiments further demonstrated that an activated *PKC1* allele, *PKC1*<sup>R398P</sup>, present on a *TRP1* plasmid, can bypass the complete loss of *SLM* function, because it allowed *slmΔ* mutant cells to grow in the absence of a *SLM1 URA3* plasmid on medium containing 5-FOA (Figure 9B). In contrast, wild-type or activated forms of the MAPK components that function downstream of Pkc1, including *BCK1* (*BCK1-20*), *MKK1* (*MKK1-DD*), and *MPK1* were unable to suppress the growth defects of Slm-

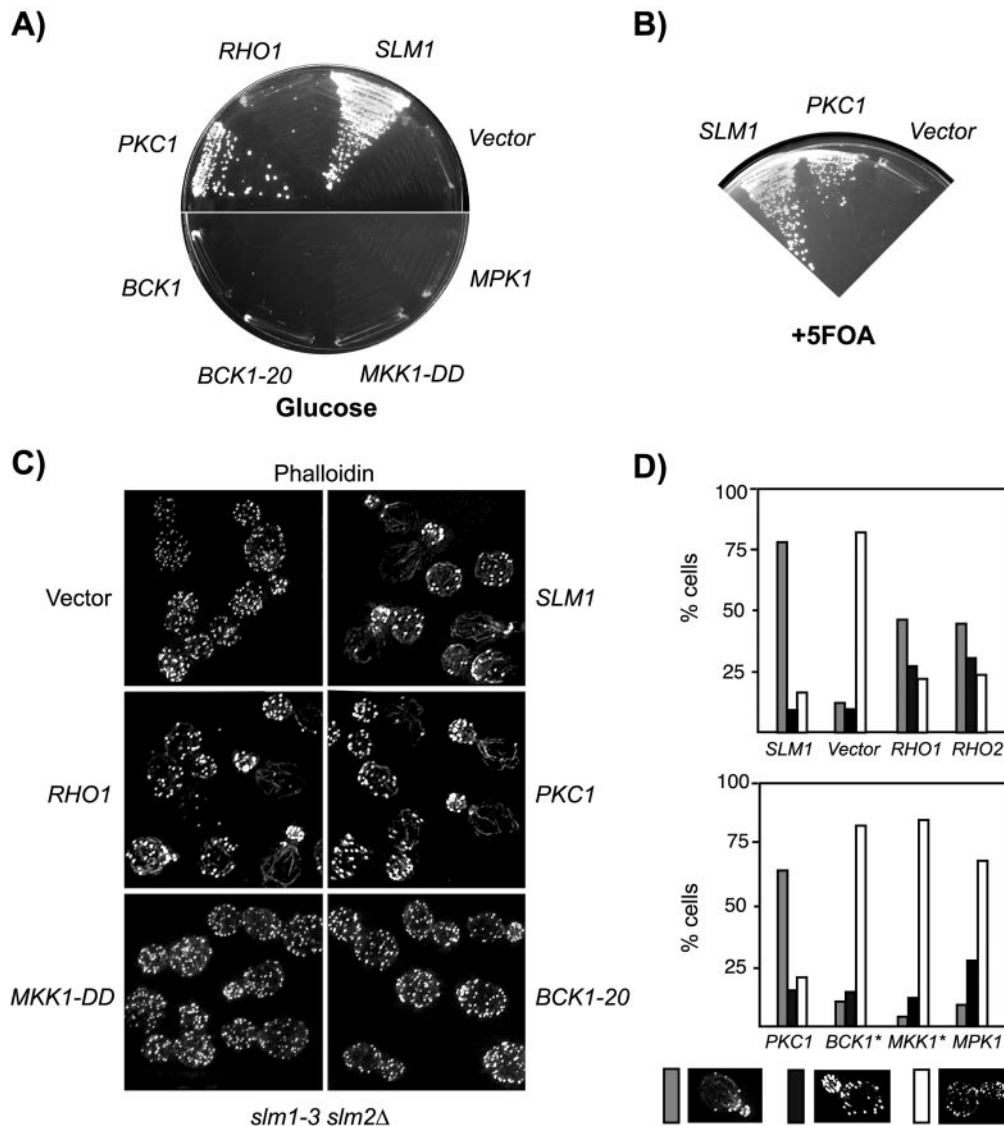


**Figure 9.** Overexpression of *PKC1* suppresses the growth and actin defects of *slm* mutants. (A) Vector alone or 2 $\mu$  plasmids containing *SLM1*, *PKC1*, *BCK1*, *MPK1*, or the activated alleles *BCK1-20* and *MKK1-DD* were transformed into strain JK513 (*slm1::KanMX slm2::HIS3/YCpURA3::GAL1-HA-SLM2*). Growth of transformants was tested on SD-Ura-Leu medium containing glucose as carbon source incubated at 30°C for 3 d. (B) Overexpression of *PKC1* bypasses *Slm* function and supports growth of strain JK512 (*slm1::KanMX slm2::HIS3/YCpURA3::GAL1-HA-SLM1*) on medium containing 5-fluoroorotic acid (+FOA). (C) Actin cytoskeleton polarization in *slm1-3 slm2Δ* cells (strain JK515) transformed with plasmids expressing the indicated genes. Cells were grown in SD-Ura-Leu medium, shifted to the nonpermissive temperature of 38°C for 3 h, fixed, and stained for F-actin by using Alexa-594-phalloidin. (D) Quantitation of the actin polarization defect of *slm1-3 slm2Δ* cells transformed with the indicated plasmids from C. Small- to medium-budded cells (~100) were scored for their actin polarization state. Cells were classified as having a polarized (gray bars), partially polarized (black bars), or depolarized (white bars) actin cytoskeleton.

depleted or of *slm1-3 slm2Δ* mutant cells grown at 38°C (Figure 9A; our unpublished data).

Overexpression of *PKC1*, but not of MAPK components also restored proper actin cable assembly and actin polarization in *slm1-3 slm2Δ* cells at 38°C (Figure 9, C and D). Overexpression of *RHO1* or expression of a constitutively activated form (our unpublished data) did not restore growth, but partially restored the proper polarization of the actin cytoskeleton in *slm1-3 slm2Δ* cells at 38°C (Figure 9, A, C, and D). Because *RHO1* reduced the growth rate in wild-type cells when overexpressed (our unpublished data), we investigated the possibility that any suppression by *RHO1* may be masked by its toxicity. However, overexpression of

the related *RHO2*, which is not toxic, conferred similar effects and partially corrected the actin defects of *slm1-3 slm2Δ* mutants at 38°C, but not the growth defects of *Slm*-depleted cells (Figure 9C; our unpublished data). Together, our data argue that activation of *Pkc1*, but not the *Pkc1*-activated MAPK signaling cascade, is sufficient to restore growth and proper actin polarization in *slm* null mutant cells.

## DISCUSSION

In this study, we show that the PH domain-containing proteins *Slm1* and *Slm2* are functionally redundant and essential for cell growth and PtdIns(4,5) $P_2$ -dependent signaling to

the actin cytoskeleton. We further demonstrate that Slm1 and Slm2 physically interact with Avo2 and Bit61 and are novel components of the TORC2 signaling complex. Slm1 (and Slm2) localize to the plasma membrane via interaction with PtdIns(4,5)P<sub>2</sub> and TORC2. In addition, Tor2 positively and possibly directly regulates the phosphorylation of Slm1 and Slm2 suggesting that Slm function is modulated in response to signals that control Tor2. Collectively, our data suggest that Slm1 and Slm2 are novel PtdIns(4,5)P<sub>2</sub> effectors that integrate inputs from the PtdIns(4,5)P<sub>2</sub> and Tor2 signaling pathways to modulate polarized actin assembly and growth. We propose that the synergistic interaction with lipid and protein ligands ensures the proper localization and regulation of Slm1 and Slm2 and is important for the compartmentalization and differential effects of PtdIns(4,5)P<sub>2</sub>-dependent signaling events.

Our data suggest that Slm1 and Slm2 respond specifically to changes in PtdIns(4,5)P<sub>2</sub> levels and thus constitute novel PtdIns(4,5)P<sub>2</sub> effectors. The lipid binding activity of Slm1 and Slm2 resides in their C-terminal PH domains, and our analysis of Slm truncation and point mutants suggests that these domains serve as membrane anchors that direct the two proteins to sites enriched in their ligand PtdIns(4,5)P<sub>2</sub>. This model is supported by a recent survey of yeast PH domains, which found that the isolated Slm1 and Slm2 PH domains localized to the plasma membrane in a manner that was dependent on PtdIns(4,5)P<sub>2</sub> synthesis (Yu *et al.*, 2004). Although the PH domain of Slm1, like other PH domains, binds to many polyphosphoinositides with no apparent selectivity *in vitro*, our data further argue that *in vivo*, Slm proteins specifically bind PtdIns(4,5)P<sub>2</sub> and that PtdIns(4,5)P<sub>2</sub> binding is essential for Slm localization and function. First, targeting of Slm1 and Slm2 to the plasma membrane is dependent upon the integrity of their PH domains and requires lipid binding activity. Second, plasma membrane association of Slm1 and Slm2 is affected by changes in PtdIns(4,5)P<sub>2</sub> levels such as in *stt4<sup>ts</sup>* and *mss4<sup>ts</sup>* mutants, and in cells that express the phosphatase SigD, which hydrolyzes PtdIns(4,5)P<sub>2</sub>. Third, manipulating cellular PtdIns(4,5)P<sub>2</sub> levels by disruption of the PtdIns(4,5)P<sub>2</sub> phosphatase *INP51* suppresses the lethality of *slmΔ* null mutant cells. Fourth, *slm1Δ* mutations are synthetically lethal with hypomorphic mutations in *STT4* or *MSS4*. Last, we demonstrate that the ability to bind PtdIns(4,5)P<sub>2</sub> is essential for Slm function, because Slm mutants that fail to bind phosphoinositides *in vitro*, also lack the ability to complement the lethality of *slmΔ* null mutant cells *in vivo*.

Although the PH domains of Slm1 and Slm2 are necessary and sufficient to direct plasma membrane targeting (Yu *et al.*, 2004; our unpublished observations), our data suggest that Slm proteins interact with a second, PtdIns(4,5)P<sub>2</sub>-independent factor at the plasma membrane that directs Slm localization to specific plasma membrane subdomains. This notion is based on the finding that Slm proteins do not uniformly localize along the plasma membrane, as do isolated PH domains that bind PtdIns(4,5)P<sub>2</sub>, but concentrate in discrete clusters. Our studies identify the TORC2 complex as a candidate PtdIns(4,5)P<sub>2</sub>-independent localization component, although we cannot rule out contribution by additional factors. Slm1 and Slm2 physically interact with the TORC2 components Avo2, Bit61, and Ybr270c, and our findings from biochemical and immunofluorescence studies are consistent with a role of these proteins in stabilizing and possibly refining Slm localization at the plasma membrane. Such combinatorial control of protein targeting by both lipid and protein determinants may be a common mechanism to regulate the localization and function of PH domain-containing

proteins. For example, the targeting of the mammalian four-phosphate adaptor proteins 1 and 2 (Fapp1 and Fapp2) to the Golgi is mediated by the simultaneous binding of their PH domains to PtdIns(4)P and the GTPase Arf1 (Godi *et al.*, 2004). PtdIns(4)P and a Golgi-localized factor also determine the targeting of the related PH domain-containing oxysterol binding proteins (Fang *et al.*, 1996; Levine and Munro, 2002). Similarly, Cla4, Boi1, and Boi2 are targeted to sites of polarized growth by both lipid-dependent and -independent mechanisms (Bender *et al.*, 1996; Hallett *et al.*, 2002; Wild *et al.*, 2004). Such a synergistic control mechanism may explain why many PH domain-containing proteins *in vitro* show little specificity in phosphoinositide recognition and bind with only moderate affinity, but still target in a specific manner *in vivo*.

Like mutants in *STT4*, *MSS4*, and *TOR2*, *slm* deletion and temperature-sensitive mutants exhibit defects in actin cable assembly and actin patch polarization. Together with our biochemical data demonstrating a direct physical interaction between Slm proteins, PtdIns(4,5)P<sub>2</sub>, and TORC2 components, these findings suggest that Slm proteins integrate inputs from Tor2 and PtdIns(4,5)P<sub>2</sub> to modulate actin cytoskeleton polarization. Consistent with the observed cytoskeletal defects, we found that two proteins, Cdc42 and Rho1, which depend on actin cables for their polarized transport to and retention at sites of growth failed to efficiently concentrate in the growing bud upon loss of Slm activity. How do Slm proteins affect actin cytoskeleton dynamics? Because the precise molecular function of Slm1 and Slm2 is at present unknown, there are multiple ways of how a loss of Slm function might lead to the observed cytoskeletal defects. Two likely possibilities are that Slm proteins either directly affect actin cable assembly or that they play a role in vesicular trafficking to the plasma membrane. Rho1 and Cdc42 are key regulators of actin cytoskeletal dynamics that promote formin-dependent actin cable assembly (Tolliday *et al.*, 2002; Dong *et al.*, 2003) and their transport to the bud is mediated by vesicular transport along actin cables (Abe *et al.*, 2003; Wedlich-Soldner *et al.*, 2003; Pruyne *et al.*, 2004). Thus, a failure or decrease in their secretion may indirectly cause the observed cytoskeletal defects in *slmΔ* mutants. Consistent with such a hypothesis, a block in secretion in several *sec* mutants also causes actin cable and actin polarization defects (Mulholland *et al.*, 1997; Pruyne *et al.*, 2004). Regardless of the precise mechanism, the phenotypic suppression of *slm* null mutants by overexpression of the cell integrity pathway component *PKC1* suggests that Slm1 and Slm2 modulate Pkc1 activity or localization. Whether Slm1 and Slm2 signaling to Pkc1 involves the upstream activator Rho1 remains to be determined. Contrary to Rho1 and Cdc42, the localization of Pkc1 to the cell cortex is independent of vesicular trafficking (Andrews and Stark, 2000), which may explain why *PKC1* is a more effective suppressor of *slm* null mutant phenotypes compared with *RHO1*.

In yeast, signaling from Tor2p to the actin cytoskeleton bifurcates at the level of Pkc1p (Delley and Hall, 1999). Interestingly, overexpression or mutational activation of components of the Pkc1-activated mitogen-activated protein (MAP) kinase cascade failed to suppress the phenotypes of *slmΔ* null mutant cells, and no synthetic lethality was observed between *slm1Δ* mutants and mutants in the MAP kinase module (our unpublished data). Thus, Slm signaling likely involves the MAP kinase independent Pkc1 signaling branch. This branch controls the cell cycle-dependent polarization of the actin cytoskeleton through yet to be defined effectors (Delley and Hall, 1999). Alternatively, and equally

consistent with our data, Slm1 and Slm2 may act in a pathway that has a function overlapping with Pkc1.

Future studies also need to address the precise roles of Slm proteins and the TORC2 components Avo2, Bit61, and Ybr270c in the Tor2 signaling pathway. Preliminary studies indicate that *SLM* overexpression does not suppress the lethality of *tor2ts* mutants and only marginally restores actin cable assembly in these mutants (our unpublished observations). However, suppression is not necessarily to be expected because most components of the TORC2 complex (except Avo2) are essential proteins (Loewith *et al.*, 2002), and mutants therein also exhibit actin defects (Loewith *et al.*, 2002). It is thus likely that Slm1 and Slm2 regulate a subset of TORC2 functions activated in response to specific environmental signals. Future identification of downstream effectors of Slm1 and Slm2 and characterization of the role of TORC2 in Slm1 and Slm2 regulation will likely provide insight into the exact molecular function of Slm proteins and reveal how they signal to the actin cytoskeleton.

Interestingly, the TORC2 complex and its modulation of PKC function may be conserved in mammalian cells. Two recent publications reported that the mammalian mTOR protein is part of a protein complex that contains the Avo3 homolog rictor (Jacinto *et al.*, 2004; Sarbassov *et al.*, 2004). This complex mediates rapamycin-insensitive mTOR signaling to the actin cytoskeleton (Jacinto *et al.*, 2004; Sarbassov *et al.*, 2004) through modulation of protein kinase C $\alpha$  (Sarbassov *et al.*, 2004), suggesting that at least some aspects of TORC2 signaling are conserved between yeast and mammals.

In summary our studies identify two novel effectors of PtdIns(4,5)P<sub>2</sub> that mediate an essential function required for growth and actin cytoskeletal organization. The yeast actin cytoskeleton is highly dynamic and quickly adapts to changes in various environmental conditions and in response to the cell cycle phase. Thus, actin dynamics is likely controlled and modulated by a network of signaling pathways that sense and integrate different stimuli. Slm1 and Slm2 contain lipid and protein binding modules and seem to function as part of such a signaling network to integrate signals from the Stt4/Mss4 and Tor2 pathways. In that way, PtdIns(4,5)P<sub>2</sub> signaling is coordinated with and dependent on other signaling pathways such as the Tor2 pathway. This, in turn, may allow the differential regulation of PtdIns(4,5)P<sub>2</sub>-dependent signaling processes in response to various environmental and intracellular stimuli.

*Note added in proof.* While this article was under review, S. Emr and colleagues (Audhya *et al.*, 2004) reported on the identification of Slm1 and Slm2 in a synthetic lethal screen with *mss4ts*. Their and our findings are in good agreement.

## ACKNOWLEDGMENTS

We thank John A. Cooper, Scott Emr, Michael Gustin, Michael Hall, Dan Johnson, David Levin, Tim Levine, Sergio Grinstein, and Daniel J. Lew for gifts of strains and plasmids; Richard Atkinson, Robin Hiesinger, and Wei-Ting Chao for help with the Deltavision Deconvolution microscope and image quantification; and Georg Halder for comments on the manuscript. This work was supported by grants GM-068098 from the National Institutes of Health and Q-1536 from the Welch Foundation (to J. K.).

## REFERENCES

Abe, M., Qadota, H., Hirata, A., and Ohya, Y. (2003). Lack of GTP-bound Rho1p in secretory vesicles of *Saccharomyces cerevisiae*. *J. Cell Biol.* 162, 85–97.

Abraham, R. T. (2002). Identification of TOR signaling complexes: more TORC for the cell growth engine. *Cell* 111, 9–12.

Alberts, A. S., Bouquin, N., Johnston, L. H., and Treisman, R. (1998). Analysis of RhoA-binding proteins reveals an interaction domain conserved in heterotrimeric G protein  $\beta$  subunits and the yeast response regulator protein Skn7. *J. Biol. Chem.* 273, 8616–8622.

Andrews, P. D., and Stark, M. J. (2000). Dynamic, Rho1p-dependent localization of Pkc1p to sites of polarized growth. *J. Cell Sci.* 113, 2685–2693.

Audhya, A., and Emr, S. D. (2002). Stt4 PI 4-kinase localizes to the plasma membrane and functions in the Pkc1-mediated MAP kinase cascade. *Dev. Cell* 2, 593–605.

Audhya, A., Foti, M., and Emr, S. D. (2000). Distinct roles for the yeast phosphatidylinositol 4-kinases, Stt4p and Pik1p, in secretion, cell growth, and organelle membrane dynamics. *Mol. Biol. Cell* 11, 2673–2689.

Audhya, A., Loewith, R., Parsons, A. B., Gao, L., Tabuchi, M., Zhou, H., Boone, C., Hall, M. N., and Emr, S. D. (2004). Genome-wide lethality screen identifies new P14,5P(2) effectors that regulate the actin cytoskeleton. *EMBO J.* 23, 3747–3757.

Bender, L., Lo, H. S., Lee, H., Kokojan, V., Peterson, V., and Bender, A. (1996). Associations among PH and SH3 domain-containing proteins and Rho-type GTPases in yeast. *J. Cell Biol.* 133, 879–894.

Cabib, E., Drgonova, J., and Drgon, T. (1998). Role of small G proteins in yeast cell polarization and wall biosynthesis. *Annu. Rev. Biochem.* 67, 307–333.

Cohen, T. J., Lee, K., Rutkowski, L. H., and Strich, R. (2003). Ask10p mediates the oxidative stress-induced destruction of the *Saccharomyces cerevisiae* C-type cyclin Ume3p/Srb11p. *Eukaryot. Cell* 2, 962–970.

Cozier, G. E., Carlton, J., Bouyoucef, D., and Cullen, P. J. (2004). Membrane targeting by pleckstrin homology domains. *Curr. Top. Microbiol. Immunol.* 282, 49–88.

Crespo, J. L., and Hall, M. N. (2002). Elucidating TOR signaling and rapamycin action: lessons from *Saccharomyces cerevisiae*. *Microbiol. Mol. Biol. Rev.* 66, 579–591, table of contents.

deHart, A. K., Schnell, J. D., Allen, D. A., Tsai, J. Y., and Hicke, L. (2003). Receptor internalization in yeast requires the Tor2-Rho1 signaling pathway. *Mol. Biol. Cell* 14, 4676–4684.

Delley, P. A., and Hall, M. N. (1999). Cell wall stress depolarizes cell growth via hyperactivation of RHO1. *J. Cell Biol.* 147, 163–174.

Desrivieres, S., Cooke, F. T., Parker, P. J., and Hall, M. N. (1998). MSS4, a phosphatidylinositol-4-phosphate 5-kinase required for organization of the actin cytoskeleton in *Saccharomyces cerevisiae*. *J. Biol. Chem.* 273, 15787–15793.

Dong, Y., Pruyne, D., and Bretscher, A. (2003). Formin-dependent actin assembly is regulated by distinct modes of Rho signaling in yeast. *J. Cell Biol.* 161, 1081–1092.

Dowler, S., Kular, G., and Alessi, D. R. (2002). Protein lipid overlay assay. *Sci STKE* 2002, PL6.

Fang, M., Kearns, B. G., Gedvilaite, A., Kagiwada, S., Kearns, M., Fung, M. K., and Bankaitis, V. A. (1996). Kes1p shares homology with human oxysterol binding protein and participates in a novel regulatory pathway for yeast Golgi-derived transport vesicle biogenesis. *EMBO J.* 15, 6447–6459.

Farkasovsky, M., and Kuntzel, H. (1995). Yeast Num1p associates with the mother cell cortex during S/G2 phase and affects microtubular functions. *J. Cell Biol.* 131, 1003–1014.

Ferguson, K. M., Kavran, J. M., Sankaran, V. G., Fournier, E., Isakoff, S. J., Skolnik, E. Y., and Lemmon, M. A. (2000). Structural basis for discrimination of 3-phosphoinositides by pleckstrin homology domains. *Mol. Cell* 6, 373–384.

Ferguson, K. M., Lemmon, M. A., Schlessinger, J., and Sigler, P. B. (1995). Structure of the high affinity complex of inositol trisphosphate with a phospholipase C pleckstrin homology domain. *Cell* 83, 1037–1046.

Foti, M., Audhya, A., and Emr, S. D. (2001). Sac1 lipid phosphatase and Stt4 phosphatidylinositol 4-kinase regulate a pool of phosphatidylinositol 4-phosphate that functions in the control of the actin cytoskeleton and vacuole morphology. *Mol. Biol. Cell* 12, 2396–2411.

Fruman, D. A., Meyers, R. E., and Cantley, L. C. (1998). Phosphoinositide kinases. *Annu. Rev. Biochem.* 67, 481–507.

Gary, J. D., Wurmser, A. E., Bonangelino, C. J., Weisman, L. S., and Emr, S. D. (1998). Fab1p is essential for PtdIns(3)P 5-kinase activity and the maintenance of vacuolar size and membrane homeostasis. *J. Cell Biol.* 143, 65–79.

Ghaemmaghami, S., Huh, W. K., Bower, K., Howson, R. W., Belle, A., De-phoure, N., O'Shea, E. K., and Weissman, J. S. (2003). Global analysis of protein expression in yeast. *Nature* 425, 737–741.

Godi, A., Di Campli, A., Konstantakopoulos, A., Di Tullio, G., Alessi, D. R., Kular, G. S., Daniele, T., Marra, P., Lucocq, J. M., and De Matteis, M. A. (2004). FAPPs control Golgi-to-cell-surface membrane traffic by binding to ARF and PtdIns(4)P. *Nat. Cell Biol.* 6, 393–404.



- Gould, K. L., Ren, L., Feoktistova, A. S., Jennings, J. L., and Link, A. J. (2004). Tandem affinity purification and identification of protein complex components. *Methods* 33, 239–244.
- Guo, W., Tamanoi, F., and Novick, P. (2001). Spatial regulation of the exocyst complex by Rho1 GTPase. *Nat. Cell Biol.* 3, 353–360.
- Hallett, M. A., Lo, H. S., and Bender, A. (2002). Probing the importance and potential roles of the binding of the PH-domain protein Boi1 to acidic phospholipids. *BMC Cell Biol.* 3, 16.
- Hama, H., Schnieders, E. A., Thorner, J., Takemoto, J. Y., and DeWald, D. B. (1999). Direct involvement of phosphatidylinositol 4-phosphate in secretion in the yeast *Saccharomyces cerevisiae*. *J. Biol. Chem.* 274, 34294–34300.
- Harrison, J. C., Zyla, T. R., Bardes, E. S., and Lew, D. J. (2004). Stress-specific activation mechanisms for the “cell integrity” MAPK pathway. *J. Biol. Chem.* 279, 2616–2622.
- Helliwell, S. B., Howald, I., Barbet, N., and Hall, M. N. (1998a). TOR2 is part of two related signaling pathways coordinating cell growth in *Saccharomyces cerevisiae*. *Genetics* 148, 99–112.
- Helliwell, S. B., Schmidt, A., Ohya, Y., and Hall, M. N. (1998b). The Rho1 effector Pkc1, but not Bni1, mediates signalling from Tor2 to the actin cytoskeleton. *Curr. Biol.* 8, 1211–1214.
- Homma, K., Terui, S., Minemura, M., Qadota, H., Anraku, Y., Kanaho, Y., and Ohya, Y. (1998). Phosphatidylinositol-4-phosphate 5-kinase localized on the plasma membrane is essential for yeast cell morphogenesis. *J. Biol. Chem.* 273, 15779–15786.
- Hurley, J. H., and Meyer, T. (2001). Subcellular targeting by membrane lipids. *Curr. Opin. Cell Biol.* 13, 146–152.
- Inagaki, M., Schmelzle, T., Yamaguchi, K., Irie, K., Hall, M. N., and Matsumoto, K. (1999). PDK1 homologs activate the Pkc1-mitogen-activated protein kinase pathway in yeast. *Mol. Cell Biol.* 19, 8344–8352.
- Ito, H., Fukuda, Y., Murata, K., and Kimura, A. (1983). Transformation of intact yeast cells treated with alkali cations. *J. Bacteriol.* 153, 163–168.
- Ito, T., Chiba, T., Ozawa, R., Yoshida, M., Hattori, M., and Sakaki, Y. (2001). A comprehensive two-hybrid analysis to explore the yeast protein interactome. *Proc. Natl. Acad. Sci. USA* 98, 4569–4574.
- Itoh, T., and Takenawa, T. (2004). Regulation of endocytosis by phosphatidylinositol 4,5-bisphosphate and ENTH proteins. *Curr. Top. Microbiol. Immunol.* 282, 31–47.
- Jacinto, E., Loewith, R., Schmidt, A., Lin, S., Ruegg, M. A., Hall, A., and Hall, M. N. (2004). Mammalian TOR complex 2 controls the actin cytoskeleton and is rapamycin insensitive. *Nat. Cell Biol.* 6, 1122–1128.
- Kamada, Y., Qadota, H., Python, C. P., Anraku, Y., Ohya, Y., and Levin, D. E. (1996). Activation of yeast PKC by Rho1 GTPase. *J. Biol. Chem.* 271, 9193–9196.
- Ketela, T., Green, R., and Bussey, H. (1999). *Saccharomyces cerevisiae* mid2p is a potential cell wall stress sensor and upstream activator of the PKC1-MPK1 cell integrity pathway. *J. Bacteriol.* 181, 3330–3340.
- Kohno, H., et al. (1996). Bni1p implicated in cytoskeletal control is a putative target of Rho1p small GTP binding protein in *Saccharomyces cerevisiae*. *EMBO J.* 15, 6060–6068.
- Kunz, J., Schneider, U., Howald, I., Schmidt, A., and Hall, M. N. (2000). HEAT repeats mediate plasma membrane localization of Tor2p in yeast. *J. Biol. Chem.* 275, 37011–37020.
- Lee, K. S., and Levin, D. E. (1992). Dominant mutations in a gene encoding a putative protein kinase (BCK1) bypass the requirement for a *Saccharomyces cerevisiae* PKC homolog. *Mol. Cell Biol.* 12, 172–182.
- Lemmon, M. A. (2003). Phosphoinositide recognition domains. *Traffic* 4, 201–213.
- Levin, D. E., Fields, F. O., Kunisawa, R., Bishop, J. M., and Thorner, J. (1990). A candidate PKC gene, PKC1, is required for the *S. cerevisiae* cell cycle. *Cell* 62, 213–224.
- Levine, T. P., and Munro, S. (2001). Dual targeting of Osh1p, a yeast homologue of oxysterol-binding protein, to both the Golgi and the nucleus-vacuole junction. *Mol. Biol. Cell* 12, 1633–1644.
- Levine, T. P., and Munro, S. (2002). Targeting of Golgi-specific pleckstrin homology domains involves both PtdIns 4-kinase-dependent and -independent components. *Curr. Biol.* 12, 695–704.
- Loewith, R., Jacinto, E., Wullschleger, S., Lorberg, A., Crespo, J. L., Bonenfant, D., Oppliger, W., Jenoe, P., and Hall, M. N. (2002). Two TOR complexes, only one of which is rapamycin sensitive, have distinct roles in cell growth control. *Mol. Cell.* 10, 457–468.
- Longtine, M. S., McKenzie, A., 3rd, Demarini, D. J., Shah, N. G., Wach, A., Brachat, A., Philippsen, P., and Pringle, J. R. (1998). Additional modules for versatile and economical PCR-based gene deletion and modification in *Saccharomyces cerevisiae*. *Yeast* 14, 953–961.
- Madaule, P., Axel, R., and Myers, A. M. (1987). Characterization of two members of the rho gene family from the yeast *Saccharomyces cerevisiae*. *Proc. Natl. Acad. Sci. USA* 84, 779–783.
- Malinska, K., Malinsky, J., Opekarova, M., and Tanner, W. (2003). Visualization of protein compartmentation within the plasma membrane of living yeast cells. *Mol. Biol. Cell* 14, 4427–4436.
- Martin, T. F. (2001). PI(4,5)P(2) regulation of surface membrane traffic. *Curr. Opin. Cell Biol.* 13, 493–499.
- Muhua, L., Adames, N. R., Murphy, M. D., Shields, C. R., and Cooper, J. A. (1998). A cytokinesis checkpoint requiring the yeast homologue of an APC-binding protein. *Nature* 393, 487–491.
- Mulholland, J., Konopka, J., Singer-Kruger, B., Zerial, M., and Botstein, D. (1999). Visualization of receptor-mediated endocytosis in yeast. *Mol. Biol. Cell* 10, 799–817.
- Mulholland, J., Wesp, A., Riezman, H., and Botstein, D. (1997). Yeast actin cytoskeleton mutants accumulate a new class of Golgi-derived secretory vesicle. *Mol. Biol. Cell* 8, 1481–1499.
- Odorizzi, G., Babst, M., and Emr, S. D. (1998). Fab1p PtdIns(3)P 5-kinase function essential for protein sorting in the multivesicular body. *Cell* 95, 847–858.
- Odorizzi, G., Babst, M., and Emr, S. D. (2000). Phosphoinositide signaling and the regulation of membrane trafficking in yeast. *Trends Biochem. Sci.* 25, 229–235.
- Page, N., Sheraton, J., Brown, J. L., Stewart, R. C., and Bussey, H. (1996). Identification of ASK10 as a multicopy activator of Skn7p-dependent transcription of a HIS3 reporter gene. *Yeast* 12, 267–272.
- Pruyne, D., Gao, L., Bi, E., and Bretscher, A. (2004). Stable and dynamic axes of polarity use distinct formin isoforms in budding yeast. *Mol. Biol. Cell* 15, 4971–4989.
- Qadota, H., Python, C. P., Inoue, S. B., Arisawa, M., Anraku, Y., Zheng, Y., Watanabe, T., Levin, D. E., and Ohya, Y. (1996). Identification of yeast Rho1p GTPase as a regulatory subunit of 1,3-β-glucan synthase. *Science* 272, 279–281.
- Reinke, A., Anderson, S., McCaffery, J. M., Yates, J., 3rd, Aronova, S., Chu, S., Fairclough, S., Iverson, C., Wedaman, K. P., and Powers, T. (2004). TOR complex 1 includes a novel component, Tco89p (YPL180w), and cooperates with Ssd1p to maintain cellular integrity in *Saccharomyces cerevisiae*. *J. Biol. Chem.* 279, 14752–14762.
- Richman, T. J., Sawyer, M. M., and Johnson, D. I. (2002). *Saccharomyces cerevisiae* Cdc42p localizes to cellular membranes and clusters at sites of polarized growth. *Eukaryot. Cell* 1, 458–468.
- Roy, A., and Levine, T. P. (2004). Multiple pools of phosphatidylinositol 4-phosphate detected using the pleckstrin homology domain of Osh2p. *J. Biol. Chem.* 279, 44683–44689.
- Sarbassov dos, D., Ali, S. M., Kim, D. H., Guertin, D. A., Latek, R. R., Erdjument-Bromage, H., Tempst, P., and Sabatini, D. M. (2004). Rictor, a novel binding partner of mTOR, defines a rapamycin-insensitive and rapamycin-independent pathway that regulates the cytoskeleton. *Curr. Biol.* 14, 1296–1302.
- Schmidt, A., Bickle, M., Beck, T., and Hall, M. N. (1997). The yeast phosphatidylinositol kinase homolog TOR2 activates RHO1 and RHO2 via the exchange factor ROM2. *Cell* 88, 531–542.
- Sciorra, V. A., Rudge, S. A., Wang, J., McLaughlin, S., Engebrecht, J., and Morris, A. J. (2002). Dual role for phosphoinositides in regulation of yeast and mammalian phospholipase D enzymes. *J. Cell Biol.* 159, 1039–1049.
- Serrano, R., Kiehlbrandt, M. C., and Fink, G. R. (1986). Yeast plasma membrane ATPase is essential for growth and has homology with (Na<sup>+</sup> + K<sup>+</sup>), K<sup>+</sup>- and Ca<sup>2+</sup>-ATPases. *Nature* 319, 689–693.
- Sherman, F., Fink, G. R., and Hicks, J. B. (1983). *Methods in Yeast Genetics*, Cold Spring Harbor, NY: Cold Spring Harbor Laboratory Press.
- Stolz, L. E., Huynh, C. V., Thorner, J., and York, J. D. (1998a). Identification and characterization of an essential family of inositol polyphosphate 5-phosphatases (INP51, INP52 and INP53 gene products) in the yeast *Saccharomyces cerevisiae*. *Genetics* 148, 1715–1729.
- Stolz, L. E., Kuo, W. J., Longchamps, J., Sekhon, M. K., and York, J. D. (1998b). INP51, a yeast inositol polyphosphate 5-phosphatase required for phosphatidylinositol 4,5-bisphosphate homeostasis and whose absence confers a cold-resistant phenotype. *J. Biol. Chem.* 273, 11852–11861.

- Takenawa, T., and Itoh, T. (2001). Phosphoinositides, key molecules for regulation of actin cytoskeletal organization and membrane traffic from the plasma membrane. *Biochim. Biophys. Acta* 1533, 190–206.
- Terebiznik, M. R., Vieira, O. V., Marcus, S. L., Slade, A., Yip, C. M., Trimble, W. S., Meyer, T., Finlay, B. B., and Grinstein, S. (2002). Elimination of host cell PtdIns(4,5)P(2) by bacterial SigD promotes membrane fission during invasion by *Salmonella*. *Nat. Cell Biol.* 4, 766–773.
- Toker, A. (1998). The synthesis and cellular roles of phosphatidylinositol 4,5-bisphosphate. *Curr. Opin. Cell Biol.* 10, 254–261.
- Toker, A., and Cantley, L. C. (1997). Signalling through the lipid products of phosphoinositide-3-OH kinase. *Nature* 387, 673–676.
- Tolliday, N., VerPlank, L., and Li, R. (2002). Rho1 directs formin-mediated actin ring assembly during budding yeast cytokinesis. *Curr. Biol.* 12, 1864–1870.
- Udan, R. S., Kango-Singh, M., Nolo, R., Tao, C., and Halder, G. (2003). Hippo promotes proliferation arrest and apoptosis in the Salvador/Warts pathway. *Nat. Cell Biol.* 5, 914–920.
- Uetz, P., *et al.* (2000). A comprehensive analysis of protein-protein interactions in *Saccharomyces cerevisiae*. *Nature* 403, 623–627.
- Valdivia, R. H., and Schekman, R. (2003). The yeasts Rho1p and Pkc1p regulate the transport of chitin synthase III (Chs3p) from internal stores to the plasma membrane. *Proc. Natl. Acad. Sci. USA* 100, 10287–10292.
- Wedaman, K. P., Reinke, A., Anderson, S., Yates, J., 3rd, McCaffery, J. M., and Powers, T. (2003). Tor kinases are in distinct membrane-associated protein complexes in *Saccharomyces cerevisiae*. *Mol. Biol. Cell* 14, 1204–1220.
- Wedlich-Soldner, R., Altschuler, S., Wu, L., and Li, R. (2003). Spontaneous cell polarization through actomyosin-based delivery of the Cdc42 GTPase. *Science* 299, 1231–1235.
- Wild, A. C., Yu, J. W., Lemmon, M. A., and Blumer, K. J. (2004). The p21-activated protein kinase-related kinase Cla4 is a coincidence detector of signaling by Cdc42 and phosphatidylinositol 4-phosphate. *J. Biol. Chem.* 279, 17101–17110.
- Yamamoto, A., DeWald, D. B., Boronenkov, I. V., Anderson, R. A., Emr, S. D., and Koshland, D. (1995). Novel PI(4)P 5-kinase homologue, Fab1p, essential for normal vacuole function and morphology in yeast. *Mol. Biol. Cell* 6, 525–539.
- Yin, H. L., and Janmey, P. A. (2003). Phosphoinositide regulation of the actin cytoskeleton. *Annu. Rev. Physiol.* 65, 761–789.
- Yu, J. W., Mendrola, J. M., Audhya, A., Singh, S., Keleti, D., DeWald, D. B., Murray, D., Emr, S. D., and Lemmon, M. A. (2004). Genome-wide analysis of membrane targeting by *S. cerevisiae* pleckstrin homology domains. *Mol. Cell.* 13, 677–688.